WATER QUALITY RESPONSES TO A SEMI-ARID BEAVER MEADOW IN BOISE, IDAHO

by

Luise Bayer Winslow

A thesis

submitted in partial fulfillment

of the requirements for the degree of

Master of Science in Civil Engineering

Boise State University

December 2021

BOISE STATE UNIVERSITY GRADUATE COLLEGE

DEFENSE COMMITTEE AND FINAL READING APPROVALS

of the thesis submitted by

Luise Bayer Winslow

Thesis Title: Water Quality Responses in a Semi-Arid Beaver Meadow in Boise, Idaho

Date of Final Oral Examination: 22 October 2021

The following individuals read and discussed the thesis submitted by student Luise Bayer Winslow, and they evaluated the student's presentation and response to questions during the final oral examination. They found that the student passed the final oral examination.

Kevin R. Roche, Ph.D.	Chair, Supervisory Committee
Anna Bergstrom, Ph.D.	Member, Supervisory Committee
Mojtaba Sadegh, Ph.D.	Member, Supervisory Committee

The final reading approval of the thesis was granted by Kevin R. Roche, Ph.D., Chair of the Supervisory Committee. The thesis was approved by the Graduate College.

DEDICATION

This thesis is dedicated to my father and grandfather, for laying the foundation.

Mange bække små gør en stor å.

ACKNOWLEDGMENTS

We do not get here alone.

I would like to thank everyone in the Stellar Engineering Graduate Program and Scholarship for their ongoing support and the incredible community they have created.

I would like to thank my teachers at Boise State University for their years of support, patience, and encouragement. I'd especially like to thank Dr. Kevin Roche and Dr. Anna Bergstrom for taking a chance on me, for keeping their cool after having to explain the same thing ten times over, and for showing up even as their own lives brought about new challenges and new life.

I would like to thank my family. Thank you, mom, for making me dinner, bringing me flowers, and checking my math. Thank you, dad, for fixing my coffee machine and for the terrible sketches and long explanations that have taught me how the world goes round. Thank you, Line and Laura, for being role models and setting the bar way higher than you needed to.

And I would like to thank Dylan for being there with bad jokes, warm hugs, endless patience and lots of love at the start and end of every day.

ABSTRACT

Beavers have been instrumental in shaping the North American riverine landscape. However, land use change and beaver trapping have caused large decreases in beaver populations, resulting in fundamental changes to river morphology, hydrology, and biogeochemical function. Effective river restoration and remediation of arid western rivers relies on a comprehensive interpretation of how beaver activity influences water quantity and quality. In this study, I compared two stream reaches with and without beaver dams in a semi-arid watershed, to quantify the effects of beaver activity on hydrology and biogeochemistry. Within each reach, I combined dilution gauging and stream tracer experiments to determine basic hydrologic measures, and analyzed water samples, using ion chromatography, to determine the concentration of major ions. Data was collected from May to July, wherein discharge rapidly declined through both reaches. Magnesium concentrations, [Mg^{2+}], decreased in both reaches, during the eight week period, and suggests [Mg^{2+}] were dependent on the contribution of groundwater relative to downgradient alluvial flow in the stream. Chloride concentrations, [Cl^-], shifted from decreasing to increasing, in both reaches during the eight week period, and were generally higher downgradient. The decreasing [Cl^-] trend suggests that high Spring flows dissolve, and transport stored chloride downstream, while the increasing [Cl^-] trend, suggests that during low Summer flows, evapotranspiration concentrates chloride in the stream water. Nitrate (NO_3^-) results indicated that the beaver meadow was a source of nitrate at low flows and suggests nitrate retention varies seasonally. The study also

provided evidence of enhanced water storage in the beaver meadow. The combined findings suggests that beaver activity increases late season water storage, and affects the timing and magnitude of nutrient cycling, in western semi-arid watersheds.

TABLE OF CONTENTS

LIST OF TABLES

LIST OF FIGURES

LIST OF PICTURES

LIST OF ABBREVIATIONS

BDA	Beaver dam analogue
BTC	Graduate College
BSU	Thesis and Dissertation Coordinator
DAF	Downgradient alluvial flow
DCEW	Dry Creek Experimental Watershed
DOM	Dissolved organic matter
ER	Ecosystem Respiration
ET	Evapotranspiration
GG	Gross Gains
HEF	Hyporheic exchange flows
HZ	Hyporheic zone
Cl, [Cl^-]	Chloride, Chloride concentration (mg/L)
CR	Control reach
CRU	Control reach upstream
IC	Ion chromatograph(y)
LG	Lower gauge
Mg, [Mg^{2+}]	Magnesium, Magnesium concentration (mg/L)
MR	Meadow reach
MRD	Meadow reach downstream
μ	Mean residence time

MRU	Meadow reach upstream
n	Manning's roughness coefficient
NO_3^-, $[NO_3^-]$	Nitrate, Nitrate concentration (mg/L)
OM	Organic matter
Q	Flow
Raz	Resazurin
Ru	Resorufin
RWT	Rhodamine by weight
USGS	United State Geological Survey

CHAPTER 1: INTRODUCTION

The North American beaver (castor canadensis) is a prolific ecosystem engineer that historically thrived across the United States and shaped the American landscape, but land use change and 19th century beaver trapping transferred control of North America's natural channels from beaver to man, with significant consequences to channel hydrology and biogeochemical function. (Wohl, 2005; Naiman et al., 1988; Wohl & Beckman, 2014).

These repercussions have raised concern within the environmental and fluvial research community who seek to restore and remediate degraded rivers. In this context beaver introduction has emerged as a viable low cost, low maintenance solution for stream restoration, with holistic benefits to channel form and function (Lautz et al., 2019; Pollock et al., 2014). But effectively leveraging the effects of beavers for stream restoration, begins by understanding how beaver activity changes channel hydrology and biogeochemical functions.

Beavers transform stream hydrology and biogeochemical function by building dams. Beaver dams impound and distribute water across and into the surrounding land creating hydrologic connections between the channel and floodplain (Westbrook et al., 2005; Wohl, 2005). Floodplain inundation substantially decreases flow velocity and increases water storage with implications to groundwater levels, ground and surface water interactions and residence time (Majerova et al., 2015; Naiman et al., 1988). Beaver dams modify biogeochemical function by enhancing anaerobic conditions and

expanding the lateral extent and interaction with reactive pathways (Briggs et al., 2013; Kuypers et al., 2018, Larsen et al., 2021).

The relationship between hydrology and biogeochemical function provides context for how beaver activity impacts water quality. Hydrology and biogeochemistry can be coupled using a mass balance of water and solute flux. But mass balances can be difficult to achieve because solute and water fluxes generally do not reach steady state conditions within the timeframe of most research projects (Larsen et al., 2021).

Studying the coupled effects of hydrology and biogeochemical function builds an understanding of how beaver activity influences water quantity and quality. Given the historical presence and abundance of beavers in North America this understanding offers insight to the historical form and function of western watersheds. It can also offer insight to how beaver activity can holistically remediate and restore present day degraded streams.

This project supplements existing research by studying a beaver meadow located within a semi-arid western watershed. The goal of the study was to quantify the relative effects of beaver activity on water quality and hydrology to expand our understanding of the link between hydrology and biogeochemical function.

CHAPTER 2: BACKGROUND

2.1 Historical Background

Imagine a natural river. Do you think of calm flows, carving its way through grassy meadows and plains? Or gushing whitewater rapids breaking the stillness of the forest? In whichever way you imagine a river, it will likely be very different from the rivers settlers saw when they first explored the vast landscape of North America. Two centuries ago, there would have been around 250 million beaver ponds throughout North America, with many ponds averaging the size of four to five acres big (Butler and Malanson, 2005; Goldfarb, 2018). This suggests that up to almost a fifth of the entire North American continent was submerged by beaver ponds. The American landscape was not only dominated by beavers but fundamentally shaped by them. Their messy marshes and vast ponds negate our modern-day image of wide snaking channels. When European settlers colonized this landscape, they found large, open spaces to build their communities on, and a plentiful population of beavers for the booming fur trade (Wohl, 2005). As the beavers were removed from the rivers and ponds, the settlers were rewarded with flat plains, containing rich, healthy soil to farm their crops and graze their livestock on. By the end of the 19th century, virtually all of North America had been colonized, and beavers had been trapped to near extinction (Naiman et al., 1988). Without consistent maintenance, the last of the beavers' once proud dams collapsed and washed away. Control of North America's natural channels shifted from beaver to man. But this corruption of the previous natural process governing rivers and their surrounding

ecosystems, threatened the plentiful environment settlers had been welcomed into, and replaced it with a potential for alluvial incision, riparian ecosystem death, and drought (Wohl, 2005).

Our modern-day depiction of a healthy water ecosystem has its foundations in retrospective analysis of this ecological history (Wohl, 2005). As the waning environmental health of North America threatened the successes of farms, forests, and natural areas, research began focusing on the degradation of western rivers, an effort that has been a priority for the last 30 years. Original remediation efforts focused on physical characteristics, rather than a holistic, functional approach (Malakoff, 2004; Rosgen, 1994). Since then, beaver re-introduction has become an increasingly popular alternative to traditional restoration approaches. The low cost and potential for long-term sustainability make beavers an attractive choice for repairing our damaged rivers (Lautz et al., 2019; Palmer & Ruhl, 2019; Pollock et al., 2014).

This approach, it should be mentioned, has not been without controversy. To this day, beavers are largely considered a nuisance to farmers and land-owners, as they break down the timber and bushes in surrounding areas, cause flooding and uncontrolled irrigation, and contaminate the springs and rivers used for drinking and livestock water (Lautz et al., 2019).

2.2 Physical Function & Characteristics

By building dams, beavers influence two main physical functions: morphology and hydrology. Beaver dams are semi-permeable structures made of wood, rocks, and sediment that span river segments. These dams prevent water from flowing freely, increasing the water depth and forming ponds in the channel behind the beaver dam

(Larsen et al., 2021). When the local water depth exceeds the bankfull, the excess water flows outward, across and into the riparian areas and floodplain (Westbrook et al., 2005). The distribution of water across the floodplain creates a beaver meadow- a complex, multi-thread system with strong hydrologic connection between the main channel and floodplain (Wohl & Beckman, 2014).

Beaver mediated inundation and lateral distribution of water across the floodplain augments surface and groundwater storage (Larsen et al., 2021). In particular beaver meadows expand the aerial extent of open surface water storage which in turn enhances groundwater infiltration (Lautz et al., 2019; Majerova et al., 2015). Groundwater infiltration raises and stabilizes the meadow's water table levels and increases ground and surface water interactions (Karran et al., 2018; Majerova et al., 2005; Wade et al., 2020).

Beaver meadows also enhance hyporheic exchange (Briggs et al., 2013). The hyporheic zone exists at the interface between the ground and surface water (Lewandowski et al., 2019, Tonina & Buffington, 2009). This is an important driver of biogeochemical reactions (Lewandowski et al., 2019). Unlike ground and surface water storage, hyporheic exchange provides transient storage at reactive scales (Lewandowski et al., 2019; Nogaro et al., 2013).

Enhanced storage and hyporheic exchange necessitate increased residence times (Larsen et al., 2021). For instance, nominal residence time is a product of nominal surface water storage (V) and meadow flow (Q), such that residence times increase directly with surface water storage:

$$\tau_{nominal} = \frac{V}{Q}$$

Furthermore, beaver meadows are characterized by modified flow velocities with different areas of fast, slow, and stagnant water. But generally beaver dams *decrease* flow velocity (Naiman et al., 1988).

Beaver mediated water storage and flow regime change temporally with seasons and attenuates high and low flows (Larsen et al., 2021). Spring snowmelt and storm events amplify surface and groundwater discharge, generally constituting seasonal peak flows. In beaver meadows peak flows are stored and slowed by being laterally distributed across the beaver meadow (Westbrook et al., 2005). This in turn delays and reduces hydrograph peaks (Puttock et al., 2017).

Seasonal low flows typically occur in the summer when evapotranspiration is highest and flows are sustained by groundwater. Beaver dams hedge low flows by raising groundwater levels and releasing stored water (Nyssen et al., 2011; Westbrook et al., 2005).

As water moves through the meadow it erodes and deposits sediments changing channel morphology over time and creating a feedback loop between morphology and flow (Pollock et al., 2014). Beaver dams disrupt longitudinal transport, modifying advective transport of sediment. Sediment storage increases and, over time, flux equilibrates in the meadow (Pollock et al., 2014; Wohl & Beckman, 2014). This provides some protection and remediation against alluvial incision (Palmer & Ruhl, 2019). Increased sediment storage also increases sediment biomass, implicating hyporheic exchange and biogeochemical processing at the reach scale (Cardinal et al., 2011; Lynch et al., 2019).

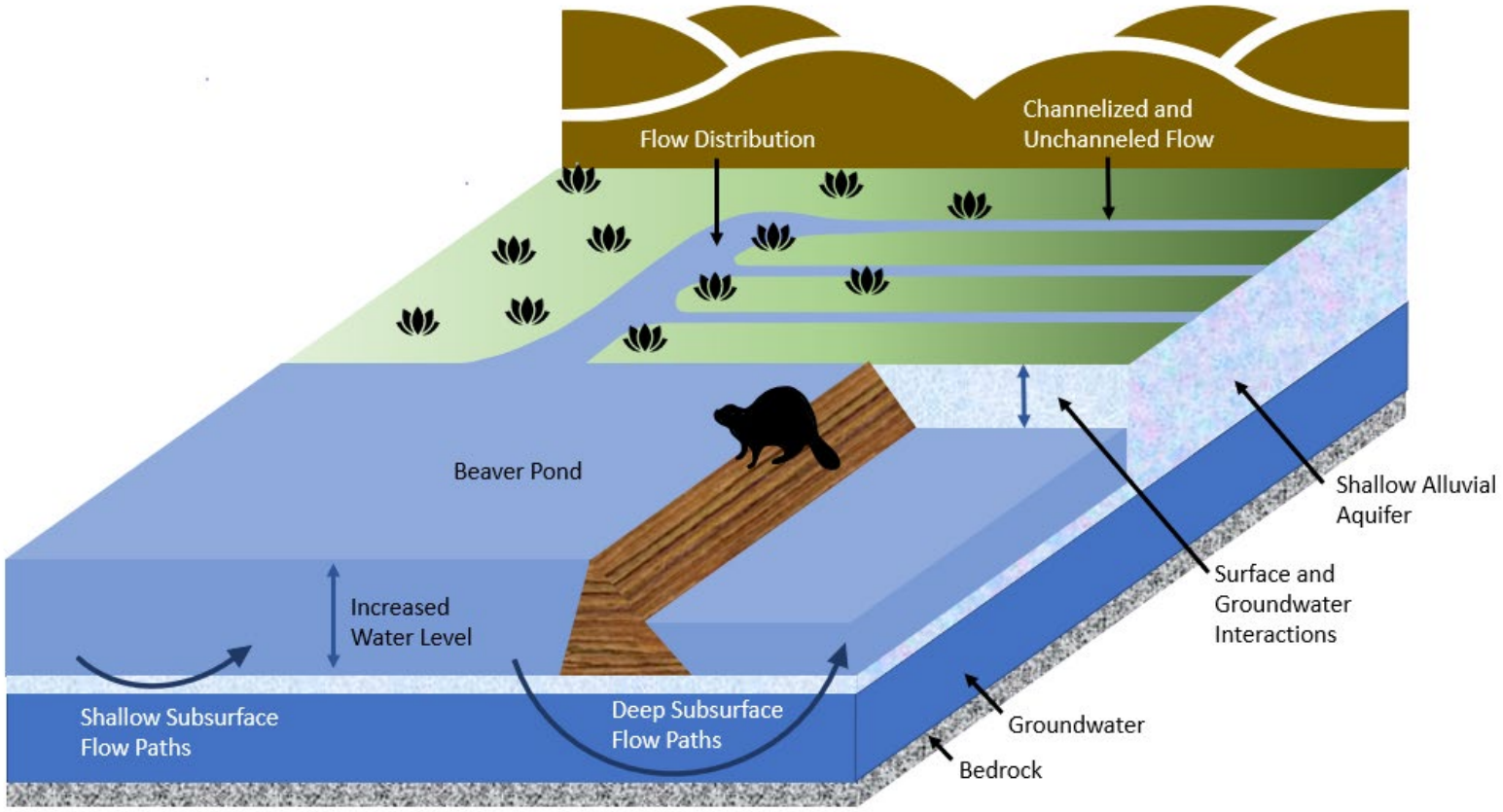

Figure 1 Conceptual model of beaver impacts to channel hydrology.

2.3 Biogeochemical Functions and Characteristics

Biogeochemistry refers to synergetic biological and geological reactions in the watershed. Beaver dams modify the biogeochemical function at the reach scale, and thus the water quality. The dams change biogeochemical pathways, spatial extent of pathways, and hydrologic connection and interaction with pathways (Larsen et al., 2021). Although many chemical changes can be studied in the changing water quality, this study focuses on beaver mediated changes to the *nitrogen cycle*.

Beaver dams generally increase organic matter storage and enhance anaerobic conditions and denitrification pathways (Larsen et al., 2021). Nitrogen rich organic matter mineralizes to ammonium (NH4) and either persists as ammonium in anaerobic conditions or is oxidized to nitrate. During nitrification ammonium (NH4) is oxidized to nitrite and then to nitrate. Both steps occur via enzymatic activity in the presence of oxygen and carbon. Denitrification (e.g. atmospheric loss) and assimilation removes nitrate from water. In anoxic conditions heterotrophic bacteria utilize nitrate as a terminal electron acceptor during respiration to atmospheric N2 (Kuypers et al., 2018). Excess nitrogen concentrations in rivers are a point of concern because they can cause eutrophication and overgrowth of invasive species (Vitousek et al., 1997). Research suggests that at the reach scale beaver meadows serve as both nitrogen sources and sinks depending on nutrient availability and residence time (Devito et al, 1989; Enisgn et al., 2005; Fisher et al., 2015; Wegener et al., 2017).

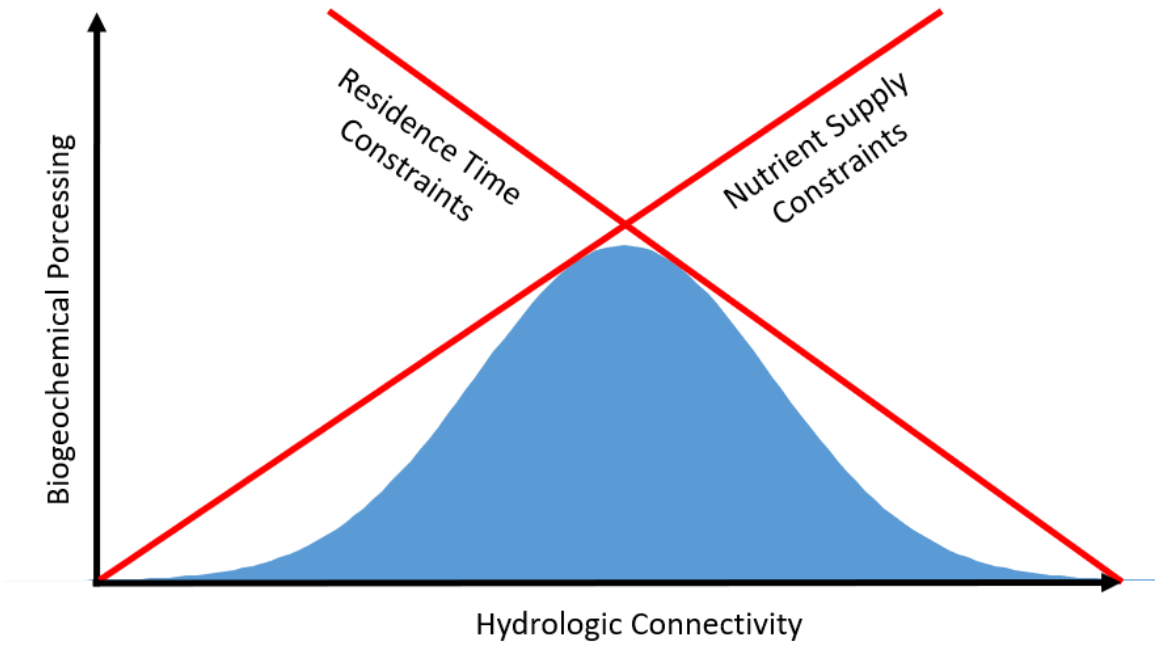

Figure 2 Diagram from Wegener et al., 2016 that conceptualizes the relationship between hydrologic connectivity and biogeochemical processing. Biogeochemical processing is constrained by nutrient delivery when connectivity is low, and by residence time when con

Geogenic solutes originate from atmospheric deposition, bedrock weathering and anthropogenic inputs (Botter et al., 2020). Weathering occurs at larger scales than individual beaver meadows but provide insight to channel hydrology and water provenance. Bedrock weathering occurs in the deep subsurface such that concentrations of geogenic solutes increase with depth (Xiao et al., 2021). Concentrations are generally studied with respect to discharge and Q-C relationships are categorized as diluting behavior, enriching behavior or chemostatic behavior. Dilution occurs when concentrations decrease with increasing discharge; enrichment occurs when concentrations increase with increasing discharge; and chemostasis occurs when solute concentrations are independent of discharge (Botter et al., 2020; Godsey et al., 2009).

Chemostasis typically occurs when water comes from the same source (Hale & Godsey, 2019; McIntosh et al., 2017)

2.4 Linking Physical and Biogeochemical Function

The relationship between biogeochemistry and hydrology is relevant for understanding how beaver meadows impact water quality, and applications for stream restoration. This relationship can be quantified using mass balances between solutes and water. But a mass balance is difficult to achieve, because water and solute fluxes are unlikely to be in steady state conditions at sub-annual scales (e.g., water) or even at annual (e.g., nitrogen) time scales (Larsen et al., 2021).

Research suggests that nutrient retention in beaver meadows varies with high and low flows (Wegener et al., 2017), but it is still unclear how much beaver dams affect seasonal trends in flow and nutrient processing. It should also be noted that the age of beaver dams may play an important role, suggesting annual and sub-annual time scales only provide transient insights to how beaver dams affect water quality (Catalan et al., 2017).

The goal of this study was to quantify the relative effects of beaver activity on water quality and hydrology (e.g. flow, residence time and water provenance) in a semi-arid western watershed. This was accomplished by tracking relative changes in surface water nitrate and geogenic solute (chloride and magnesium) concentrations, flow, mean residence time, storage, and gross gains and losses through an upstream beaver meadow and through a downstream confined control reach. The study was conducted from spring to summer, when the main channel discharge rapidly decreased. The study's hypotheses and related reasonings are summarized in Table 1.

Table 1 Hypotheses

1. *There is no change in magnesium and chloride concentrations between the upstream and downstream sampling sites within each reach. There is a greater reduction in nitrate concentration through the beaver meadow than the control reach.*

   Changes in the concentration of geogenic solutes like magnesium and chloride are typically the result of weathering. Weathering occurs at larger spatial scales than individual beaver meadows and is unlikely to result in significant changes to magnesium and chloride concentrations at the reach scale.

   Beaver meadows enhance anaerobic conditions and support denitrification pathways. Denitrification decreases surface water nitrate concentrations such that there is a greater reduction in nitrate through the beaver meadow than the control reach.

---

2. *Magnesium and chloride concentrations in the beaver meadow and the control reach increase as discharge in the main channel decreases. Relative nitrate reduction through the beaver meadow is reduced as main channel's discharge through the beaver meadow is reduced.*

   Magnesium and chloride concentrations are typically higher in the subsurface where chemical weathering takes place. Spring discharge is dominated by snowmelt. As discharge decreases in summer, relatively more water is contributed from the subsurface.

   Decreases in flow reduce the opportunity for nitrate to interact with reactive pathways and flow paths, such that the reduction in nitrate concentrations through the beaver decreases when discharge decreases.

CHAPTER 3: STUDY AREA

3.1 Site Description

The study was conducted within the lower reaches of the 28 sq.km, semi-arid Dry Creek Experimental Watershed (DCEW) from May to July 2021. The watershed is located approximately 16 miles north of Boise, Idaho. The headwaters of Dry Creek begin at an elevation of 2100 m ASL, near the Bogus Basin Ski Resort at Shafer's Butte and within the Boise National Forest. The Experimental Watershed outlet is located at the junction of Dry Creek and Bogus Basin Road, but the creek continues southwest to its confluence with the Boise River. A series of beaver dams exist about 2 miles upstream of the junction, within lower Dry Creek.

Dry Creek is a small intermittent stream, where the creek's discharge is dominated by spring snowmelt. Discharge typically peaks in May followed by a rapid return to baseflows in August. Shingle Creek, a perennial tributary located about 2 miles from the junction, and various smaller intermittent streams also flow to Dry Creek. Spring offers cool rains leading to hot and dry summers where evapotranspiration plays an important role in reducing streamflow (Geisler, 2015). The lower section of the Experimental Watershed is characterized by grasses, deciduous trees and shrublands, including wild roses, syringa (Philadelphus lewisii) and sagebrush (Artemisia tridentata). The lower DCEW resides on private land, and herds, of about 10-20 cattle, regularly graze the riparian zone of Dry Creek in spring and summer.

The DCEW has been characterized by researchers from Boise State University's Geosciences department and the College of Idaho's Biology department over the past 20 years. Boise State University's mission in Dry Creek is to provide continuous and spatially distributed hydrologic data. BSU has established 7 active stream gauging sites across the watershed, including the Lower Gauge site with telemetered discharge estimates. Boise State's public repository of historical discharge data was used in selecting the study period, and best calibration and data collection practices. The College of Idaho's mission in Dry Creek is to monitor the movements and behaviors of the Red Band Trout population in Dry Creek.

I selected two study reaches within the experimental watershed: the meadow reach (MR) and the control reach (CR). The MR is heavily characterized by beaver activity, with several dams and a multithread channel structure. The CR represents a section of channel unimpacted by beavers and serves as a comparison to the MR. Reach lengths were selected such that residence times were approximately the same.

The MR is located just below the confluence with Shingle Creek and extends approximately 190 m. from the upstream sampling station (MRU, Pictures 3 and 4) to the downstream sampling station (MRD, Pictures 1 and 2). The channel is situated at the bottom of a wide valley. The reach was heavily characterized by beaver activity during the study period. MRU and MRD were both easily accessed from a nearby foot trail.

The CR is located about 1 mile downstream from the MR and is approximately 392 ft. long between the upstream sampling site (CRU, Pictures 7 and 8) to the reach outlet (LG, Pictures 5 and 6). CR typically sustains flows from early fall to early summer, but dries in mid summer (C. Walser, personal communication, October 21, 2020), as was

the case during the study period. CRU is easily accessed from the footpath near the northern banks, but steep foothills slope upward along the southern bank. The channel becomes increasingly confined with distance downgradient, as it enters a narrow valley with steep sloping hillsides. LG can be difficult to spot from the footpath, due to concentrated vegetation growth on the narrow channel banks and can only be accessed by climbing down the steep hillsides. LG is an established site previously set up by Boise State University's Geosciences Department. The approximate locations of LG and CRU relative to MRD and MRU can be seen in Figure 3.

Picture 2 **Upstream view of MRD**

Picture 1 **Downstream view of MRD**

Picture 4 **Upstream view of MRU**

Picture 3 **Downstream view of MRU**

Picture 6 Upstream view of LG

Picture 5 Downstream view of LG

Picture 8 **Downstream view of CRU**

Picture 7 **Upstream view of CRU**

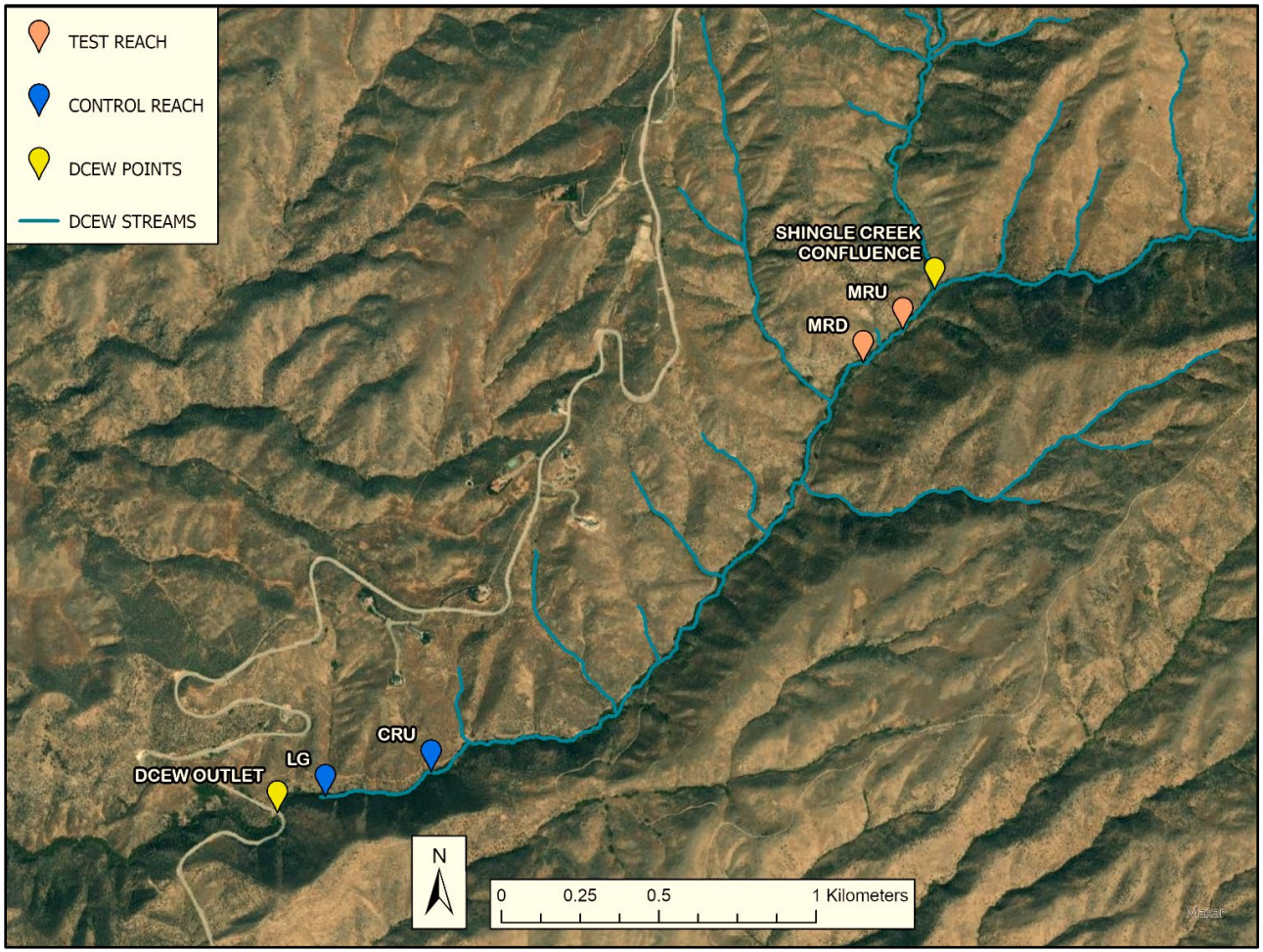

Figure 3 Sample sites LG and CRU along the CR (no beaver activity) and sample sites MRD and MRU along the MR (with beaver activity). Dry Creek outlet at the junction with Bogus Basin Rd. and the confluence with Shingle Creek are also shown.

3.2 Continuous Data

Continuous data was used for context and compared to new data. Continuous data from the DCEW was obtained from the DCEW website and is freely available to the public as CSV files. Historical stream data were downloaded for LG from the years 2017, 2018, 2019 and 2020. Stream data at LG includes discharge, temperature and flow. The discharge is calculated using rating curves maintained by Boise State University's College of Geosciences. Stage measurements were recorded using an Odyssey Capacitance Water Level Logger ODYWL (Christchurch, NZ) with a resolution 0.8 mm. Conductivity and temperature were measured using a Campbell Scientific Conductivity Sensor CS547A (Logan, UT, USA) with a resolution of 0.001 mS/cm and Campbell Scientific A547 Data Logger (Logan, UT, USA). The data is sent to Boise State University via onsite telemetry (McNamara and Aishlin, 2017, 2018, 2019, 2020).

Historical data from the DCEW at LG indicates stream discharge is dependent on winter and spring precipitation and snowmelt. Discharge generally peaks in early April, with a rapid decline to baseflow or drying in August. Flows increase again in September, as ambient temperature and evapotranspiration decrease. During the study period, from May to August, flows typically decrease from about 170-550 L/s in late May to about 0-30 L/s in early August at LG, with the exception of increases during major rainfall events.

Figure 2 compares the 2021 precipitation hyetograph to discharge at LG. The figure shows fluctuations in discharge from January to February with a few interspersed precipitation events. There is a steady increase in discharge from March to May as the snow melts, as well as sporadic increases in discharge due to rain fall events. Independent

of a major rainfall event in mid June, flows steadily decrease until September. From September to December temperatures decrease, such that discharge steadily increases as a function of reduced evapotranspiration rather than precipitation. During this time minor precipitation events result in temporary increases in discharge.

Figure 3 plots historical discharge measurement from 2017 to 2020 at LG from late May to early August. The figure shows a general decrease in discharge from late May to early June. During this time flows peak, particularly in 2019, as a result of rainfall events. In 2020 and 2017 there is an increase in discharge around mid June, a similar increase takes place around the end of June in 2018 and 2019. Following the surcharge flows decrease and converge to between 9.70 L/s and 33.05 L/s in early August.

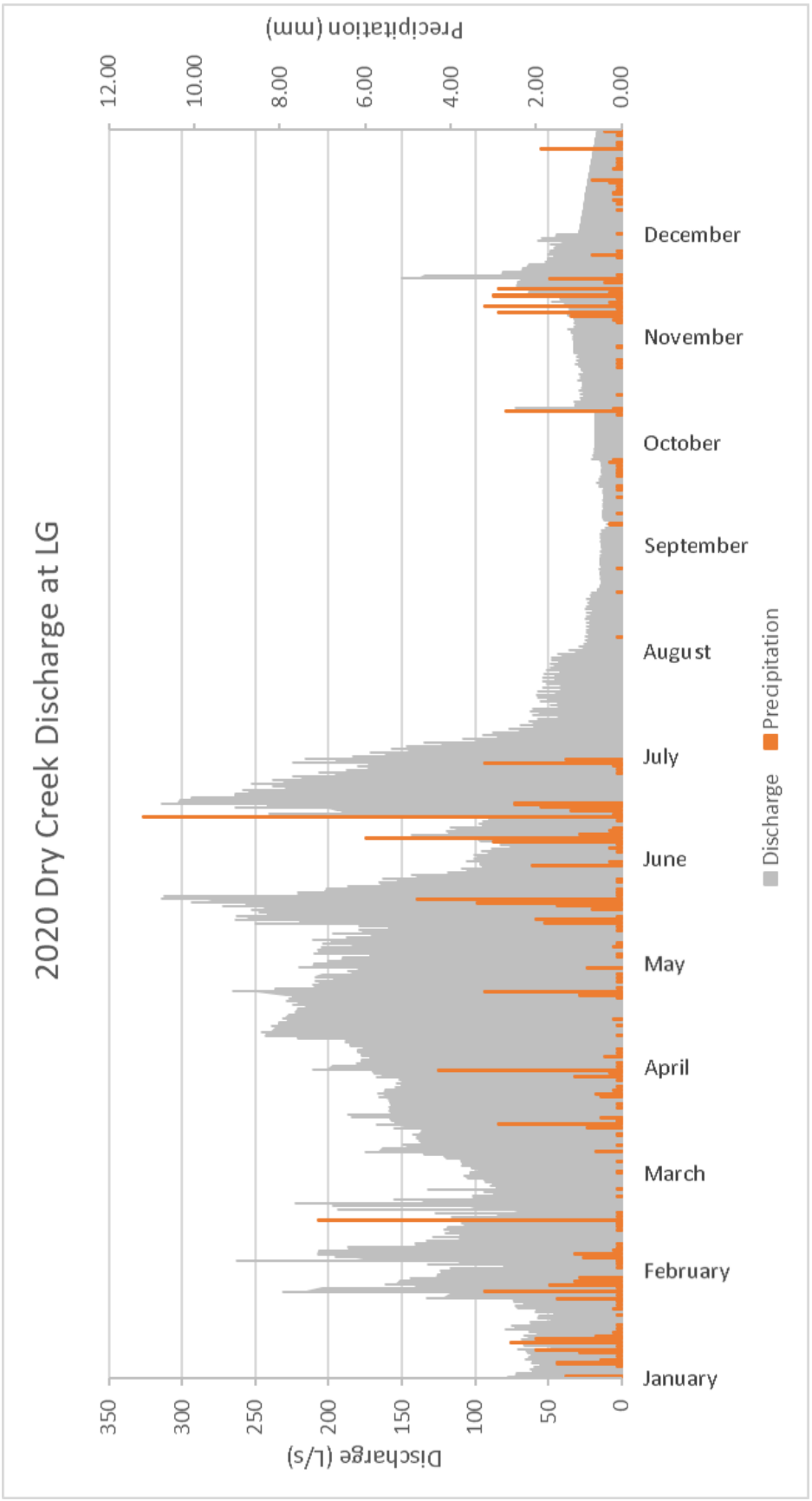

Figure 4 Historical discharge and precipitation records at LG from 2020.

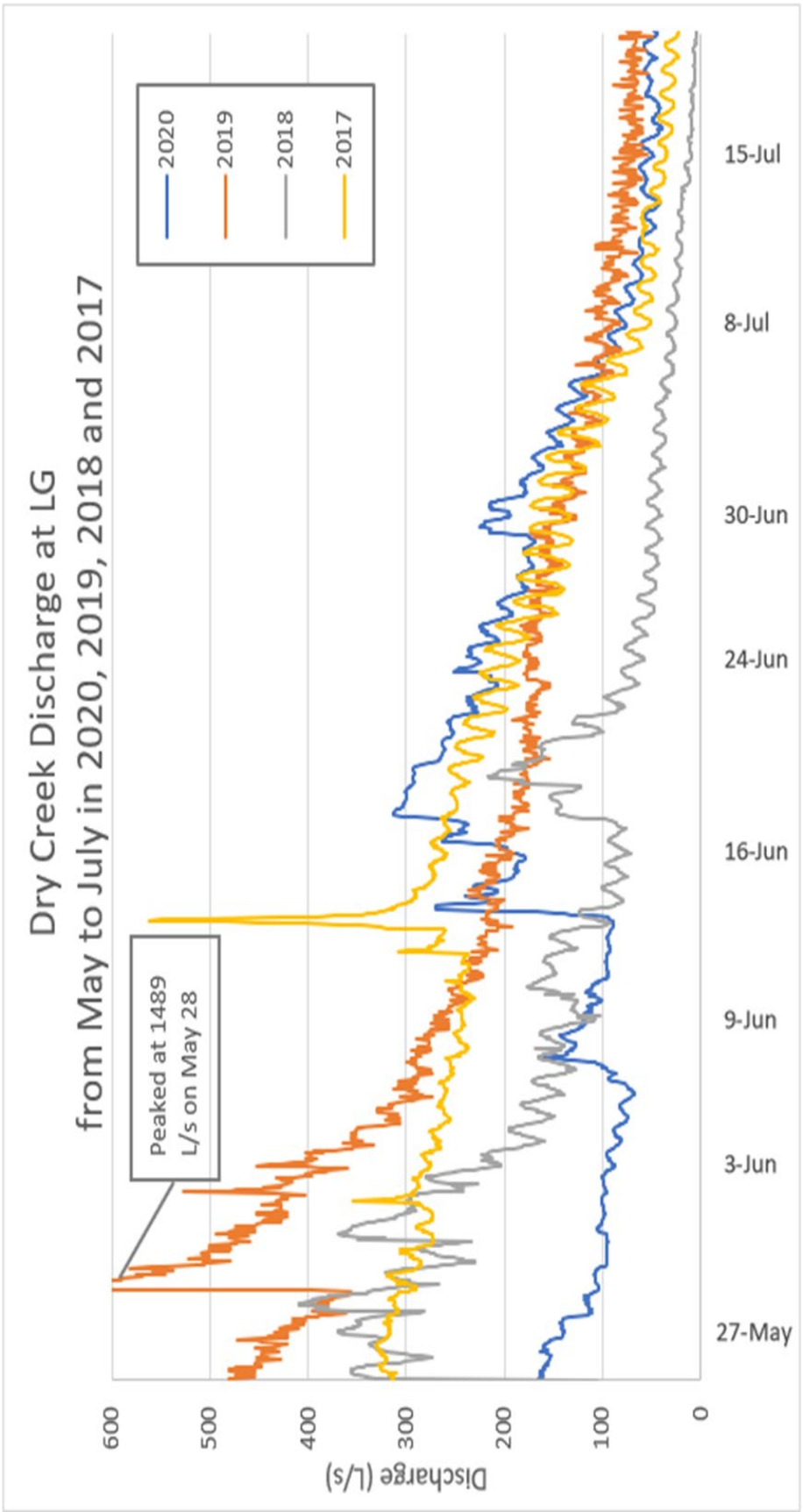

Figure 5 **Historical discharge measurements at LG from late May to late July in 2020, 2019, 2018 and 2017.**

CHAPTER 4: METHODS

4.1 Data Collection and Experimentation

I conducted the experiment during an eight week period between 05/27/21 and 07/15/21. During this period, I collected data on a weekly basis on either Wednesdays or Thursdays. Data are categorized as historical data, dilution gauging, water quality sampling and tracer experiments. The schedule is shown in Table 2 and each category is discussed in further detail below.

Table 2 Data Collection schedule for dilution gauging, water quality sampling and tracer experiments.

Week	1	2	3	4	5	6	7	8
Date	5/27	6/03	6/09	6/16	6/24	6/30	7/08	7/15
Dilution Gauging	X	X	X	X	X	X	X	X
Water Quality Sampling	X	X	X	X	X	X	X	X
Tracer Experiment		X			X			X

4.1.1 Dilution Gauging

I conducted dilution gauging experiments at the upstream and downstream locations of each study reach (Turnipseed & Sauer, 2010). I instantaneously injected potassium bromide (KBr), dissolved in stream water, 5-10 m upstream of each sampling site to promote full mixing. Conductivity was then measured at the sampling sites using an Xylem EXO 3 Multiparameter Sonde 599503 (Yellow Springs, OH, USA) equipped with conductivity and temperature probes. The sonde was deployed for approximately 10 minutes, at either 3- or 10-seconds intervals. The sonde measured background

conductivity, the arrival of KBr (breakthrough curve) and the return to background levels. Dilution gauging was completed in order from the downstream most site (LG) to the upstream most site (MRU). The gauging schedule and corresponding KBr masses are shown in Table 3.

Table 3 KBr mass in grams injected at each sampling point during weekly dilution gauging experiments.

Week	1	2	3	4	5	6	7	8
Date	5/27	6/03	6/09	6/16	6/24	6/30	7/08	7/15
MRU	100.45	99.80	99.61	99.96	100.12	98.68	97.00	99.03
MRD	99.86	100.56	100.52	100.36	99.91	96.49	92.17	100.14
CRU	100.17	99.88	100.20	100.67	99.99	96.60	96.43	99.36
LG	100.37	100.01	100.78	99.65	100.04	96.85	99.08	99.05

4.1.2 Conservative Tracer Experiment

I conducted tracer experiments on weeks 2, 5 and 8 by instantaneously injecting Rhodamine-WT (RWT) at the upstream sampling sites (MRU and CRU). The concentration time series, or breakthrough curve (BTC), of RWT was then measured at the downstream sampling sites (MRD and LG) using the EXO 3 Sonde equipped with an RWT Sensor. Sampling intervals were adjusted dynamically based on the measured concentration and varied from 30 seconds to 10 minutes during each recording. The sonde was deployed prior to injection at both downstream sampling points. At MRD the sonde was left overnight (roughly 18 hours) while at LG the sonde was left for approximately 2-3 hours. Rhodamine injections were routinely completed at CR before repeating the experiment at the upstream MR (Kilpatrick & Wilson, 1989; Knapp et al., 2017).

The EXO 3 Sonde was calibrated in the lab prior to field measurements. For RWT calibration known solutions of RWT and DI water were mixed and measured using the EXO 3 Sonde (see Appendix A).

Table 4 Rhodamine mass in grams injected at MRU and CRU during each tracer injection event.

Week	2	5	8
Date	6/03	6/24	7/15
MRU	98.70	59.55	50.08
CRU	61.60	34.85	31.19

4.1.3 Water Sampling

Water grab samples were collected weekly at each sampling site (MRU, MRD, CRU and LG) to analyze concentrations of anions and cations, including the nutrient NO_3^-. Water samples were field filtered through 0.45µm glass fiber filters into 60mL polyethylene bottles. Bottles were triple rinsed with both DI water and filtered stream water prior to sampling. Samples were transported to the lab and stored at 4°C until analysis (Lurry & Kolbe, 2000).

4.2 Data Analysis

4.2.1 Stream Discharge

I used the dilution gauging BTCs to calculate discharge at each site. I began by background correcting the recorded specific conductivity and converting to concentration of KBr using a 1:1.4 scaling factor. The scaling factor was determined in the laboratory by calibration with stream water (See Appendix A).

Discharge (Q) was calculated from the breakthrough curve using the equation below:

$$Q = \frac{KBr_{mass}}{\int_0^{t_{final}} [KBr](t)dt}$$

where KBr_{mass} is the mass of KBr added at the injection site and [KBr] is the background corrected KBr concentration. Time (t) was measured from the initial injection of KBr where $t = 0$, and $t = t_{final}$ is the time at which [KBr] had returned to background. Combined reach scale discharge ($Q_{average}$) was calculated as the average of upstream and downstream discharge.

$$Q_{average} = \frac{Q_{upstream} + Q_{downstream}}{2}$$

Net discharge was calculated using the equation below:

$$Q_{Net} = Q_{downstream} - Q_{upstream}$$

On June 30th the sonde was pulled too early at LG and failed to capture the entire breakthrough curve. The discharge at LG was estimated using the equation below:

$$Q_{LG_8} = Q_{CRU_8} + \frac{\sum_1^7 Q_{LG_n} - Q_{CRU_n}}{7}$$

where *n* is the week number from week 1 to week 8. In this case the discharge at LG on week 8 was calculated by adding the average difference between CRU and LG discharge, from weeks 1 through 7, to the CRU flow in week 8.

4.2.2 Mean Residence Time and Mass Recovery

I used the concentration time series data from the conservative tracer experiments to calculate mean residence time (μ) and rhodamine mass recovery (Yu-Chen et al., 2003). The fluorescence values were background corrected by subtracting the background fluorescence during each tracer event from the recorded data. Background

fluorescence was taken as the initial fluorescence recorded at the site, at time of deployment.

Mean residence time (μ) was calculated from the breakthrough curve using the equation below:

$$\mu = \frac{\int_0^{t_{final}} [RWT](t)\mathrm{dt}}{\int_0^{t_{final}} [RWT]\mathrm{dt}}$$

where $[RWT]$ is the background corrected RWT concentration. Time (t) was measured relative to the initial injection time of rhodamine where $t_0 = 0$ and $t_f =$ time of the final datapoint.

The fraction mass recovery (f) of each rhodamine injection was calculated using the equation below:

$$f = \left(\frac{Q_{average}}{RWT_{mass}}\right) \int_0^{t_{final}} [RWT]dt$$

where RWT_{mass} is the mass of RWT injected.

The sonde batteries failed on week 8 at LG, rendering the CR RWT data unusable. The μ within the CR on week 8 was estimated using Manning's equation (Worrall et al., 2014). See the Appendix A for more information.

4.2.3 Gross Gains and Storage

I used the discharge, mean residence time and mass recovery results to calculate gross gains and storage. Gross gains were calculated using the equation below and were based on mass recovery and discharge results (Exner-Kittredge et al., 2014; Payn et al., 2009):

$$Q_{gain} = \left(Q_{upstream} - Q_{downstream}\right) + \left(Q_{average}\right) * (1 - f)$$

Gross gains and losses were not calculated for week 8 at CRU because I was unable to calculate f (see Section 4.2.2).

Storage was calculated using the equation below and were based on μ and discharge results (Briggs et al., 2009):

$$S = Q_{average} * \mu$$

4.2.4 Ion Concentrations

I analyzed the stored water samples for [Cl^-], [Mg^{2+}], and [NO_3^-] using a Metrohm Compact IC Plus chromatograph. After calibration, the Metrohm MagIC Net software identified ion components in the chromatogram and integrated the chromatogram peak to find the ion concentration, based on the software's default analysis algorithm.

CHAPTER 5: RESULTS

5.1 Stream Discharge

Discharge (Q) measured during the study period at all four sites varied from 60.4 L/s to 0.6 L/s, decreasing monotonically across the study period (Figure 6). During weeks 1, 6, 7 and 8 channel discharge in the MR surpassed channel discharge in the CR, such that from week 2 to 5 channel discharge in CR surpassed channel discharge in MR.

5.1.1 Meadow Reach

During the study period flows from MRU decreased from 60.4 L/s to 2.0 L/s. 60.4 L/s, recorded in week 1, was the highest discharge of any site during the study period, while 2.0 L/s was the highest discharge of any site recorded in week 8. The largest decrease in flows took place between week 1 and week 2 of the study period. From week 2 to week 8 changes to flow continued to drop, but at a slower rate. Flows at MRD decreased from 58.0 L/s to 1.7 L/s with the largest drop occurring between weeks 1 and 2. During weeks 2, 3, 4 and 5 MRD had the lowest flows of any site. MRD flows began converging with MRU flows starting in week 5.

Average flows in the MR decreased by 57.4 L/s and ranged from 59.22 L/s to 1.85 L/s. The main channel of the reach remained connected during the study period, but side channels dried by week 5. Because flows at MRU were consistently higher than flows at MRD, the MR was a net sink of water with an average net loss of 2.9 L/s and a standard deviation of 2.0 (Figure 9). The figure shows the greatest net loss occurs on weeks 2, 4 and 5, with the smallest water loss in weeks 7 and 8.

5.1.2 Control Reach

At CRU flows decreased from 55.6 L/s to 0.8 L/s at CRU with largest decrease occurring from week 1 to week 2. CRU had the lowest flows of any site during weeks 1, 6, 7 and 8, with the lowest flow of any site during the study period of 0.8 L/s in week 8. Flows at LG decreased from 56.1 L/s to 0.9 L/s with the largest drop occurring between weeks 1 and 2. LG displayed the highest flows of any site during weeks 2, 3, 4 and 5.

The average flow in the CR decreased by 55.0 L/s and ranged from 55.8 L/s to 0.9 L/s (Figure 7). The main channel remained connected throughout the study period, but LG dried shortly after the conclusion of the study, leaving intermittent stagnant pools. The greatest net gains occurred on weeks 1, 2 and 7, with the smallest water gain in weeks 2 and 8 (Figure 8).

Table 5 Discharge (L/s) at each sampling site during the study period.

Week	1	2	3	4	5	6	7	8
Date	5/27	6/03	6/09	6/16	6/24	6/30	7/08	7/15
MRU	60.41	36.31	30.61	23.18	16.12	11.73	6.30	2.02
MRD	58.03	31.70	28.45	17.95	11.17	9.03	5.68	1.69
CRU	55.58	37.64	30.80	25.97	17.02	8.43	2.37	0.84
LG	56.11	37.66	31.35	26.30	17.31	8.77	2.86	0.90

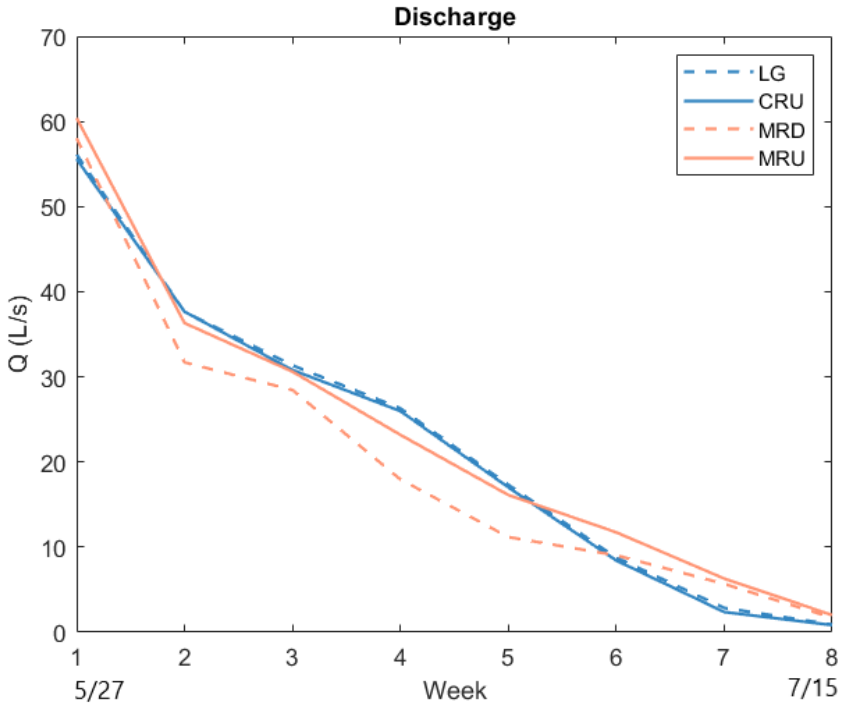

Figure 6 Volumetric discharge measurements at LG, CRU, MRD and MRU from each sampling date of the experimental period. The CR is bracketed by LG and CRU and the MR is bracketed by MRD and MRU.

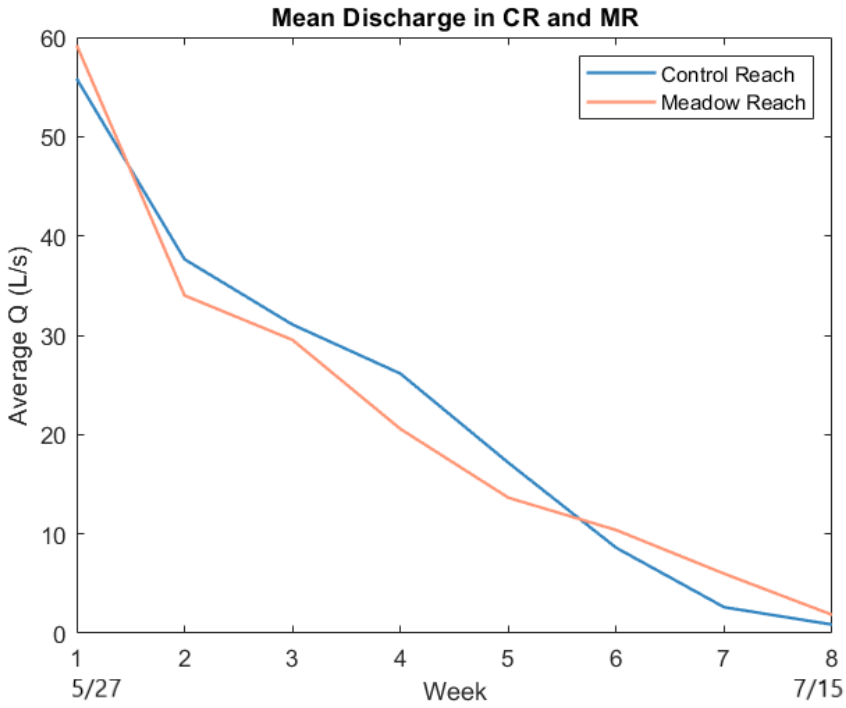

Figure 7 Mean reach flow in the MR and the CR.

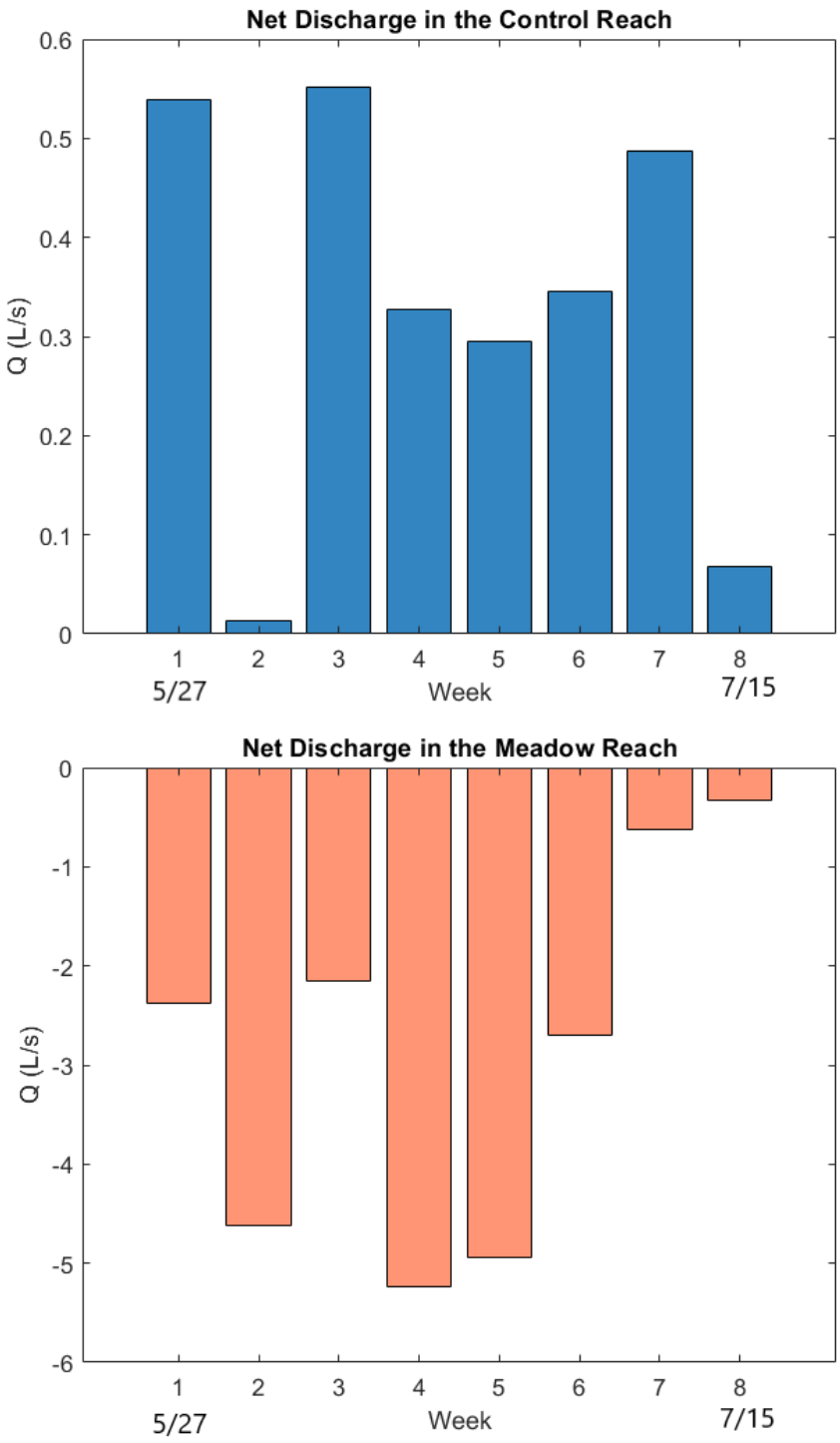

Figure 8 Net discharge in the MR and CR.

5.2 Mean Residence Time and Mass Recovery

Mean residence time in the MR rose from 42 minutes in week 2, to 56 minutes in week 5 and to an estimated 168 minutes in week 8 (Table 5). The μ within CR rose from 34 minutes in week 2, to 55 minutes in week 5. Mass recovery ranged from about 50 - 70% in the MR and stayed at about 90% in the CR (Table 5). Note that f was not calculated for the CR on week 8.

Table 6 Mean residence time in the MR and the CR on weeks 2, 5 and 8. Recall mean residence time on week 8 in the CR was estimated using Manning's equation.

Week	μ in MR (min)	f in MR (%)	μ in CR (min)	f in CR (%)
2	42	91	34	90
5	56	90	55	73
8	168	73	[146-152]	-

5.3 Gross Gains and Storage

The CR had a gross gain of 3.47 L/s and 1.93 L/s in weeks 2 and 5, respectively (Table 6). The calculated gross gains in MR were negative for weeks 2, and 5 and rose to 0.61 L/s in week 8. Negative gross gain values indicate a source of error because net loss exceeds gross loss. Note gross gains were not calculated for week 8 in the CR.

Storage ranged from 0.0984 m^3/m to 0.454 m^3/m in the MR and was higher than storage in the CR (Table 7). Note storage for week 8 was based on the range of estimated values of μ at CRU on week 8.

Table 7 Gross gains and losses in the MR and CR.

Week	MR Gross Gains (L/s)	MR Gross Losses (L/s)	CR Gross Gains (L/s)	CR Gross Losses (L/s)
2	-1.34	3.28	3.48	3.46
5	-1.25	3.70	1.93	1.64
8	0.61	0.94	NA	NA

Table 8 Water storage in the MR and CR.

Week	MR Storage	MR Length	MR Storage	CR Storage	CR Length	CR Storage
	1000 L	m	m^3/m	1000 L	m	m^3/m
2	86.3	190	0.454	77.5	392	0.198
5	45.6	190	0.240	56.7	392	0.145
8	18.7	190	0.0984	[7.62-7.84]	392	[0.0194-0.0200]

5.4 Ion Concentrations

Concentration discharge (Q-C) and concentration time (Q-t) plots were developed for chloride, magnesium, and nitrate at each site (Figures 4-9).

5.4.1 Chloride

$[Cl^-]$ ranged from 1.91 ppm at CRU to 1.14 ppm at MRU. $[Cl^-]$ was higher in the CR than the MR on each sampling date except for week 8. On week 8 $[Cl^-]$ at MRD peaked at 1.70 ppm. This datapoint was seemingly an outlier and was therefore not included in analysis of temporal trends in $[Cl^-]$. $[Cl^-]$ concentrations decreased for approximately the first 4 to 6 weeks, such that $[Cl^-]$ decreased with flow. After week 6, when flows were below 20 L/s, $[Cl^-]$ began increasing while flows kept decreasing.

5.4.2 Magnesium

Magnesium concentrations ranged from 2.81 ppm to 1.81 ppm and were higher in the CR than the MR on each sampling date. There was a positive relationship between $[Mg^{2+}]$ and main channel discharge, such that $[Mg^{2+}]$ consistently decreased as main channel discharge decreased.

5.4.3 Nitrate

Nitrate concentrations ranged from below the detection limit (0.05 ppm) to 0.76 ppm at LG in week 1. $[NO_3^-]$ decreased rapidly at MRU, CRU and LG between weeks 1

and 4 such that all three were near the detection limits between weeks 4 and 8. [NO_3^-] at MRD remained detectable until week 8, such that [NO_3^-] was generally higher at MRD than at MRU.

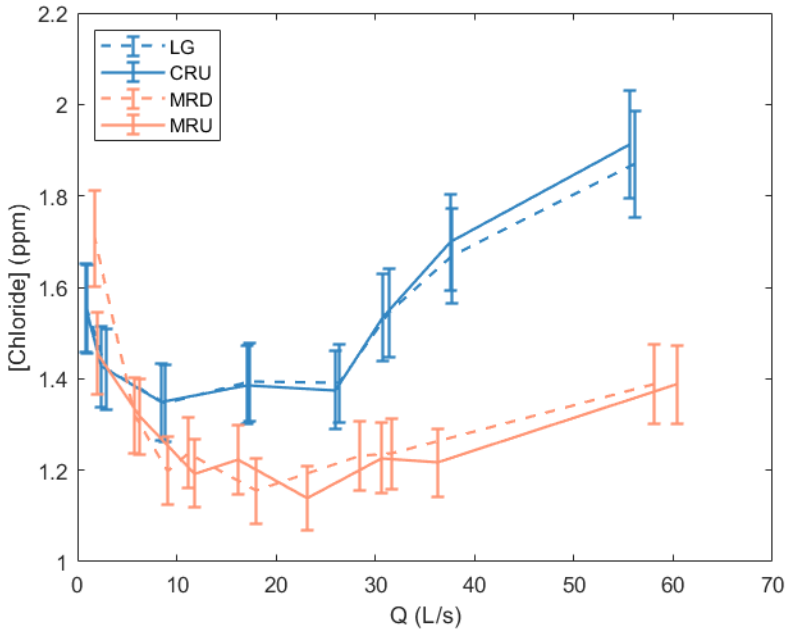

Figure 9 Mean discharge and dissolved [Cl⁻]. Generally [Cl⁻] decreased with discharge, but at flows below ~10 L/s [Cl⁻] increased with discharge.

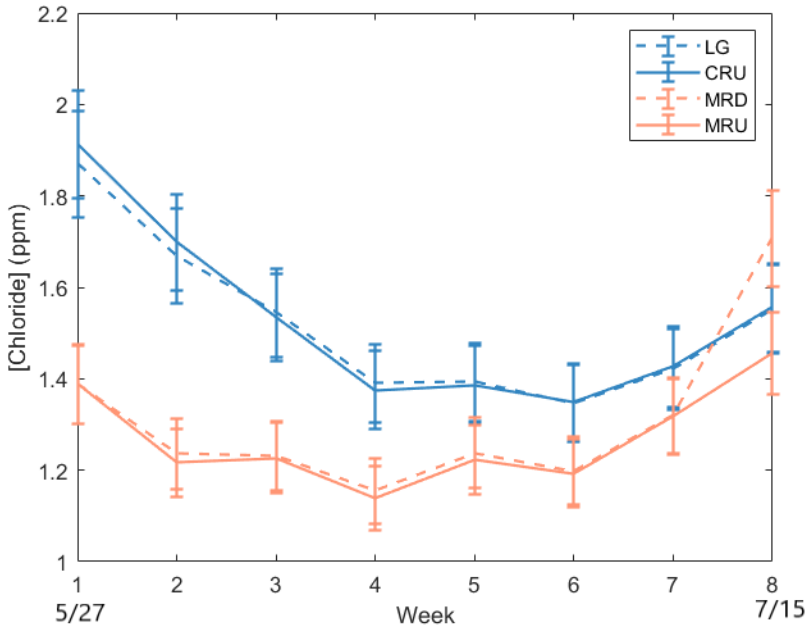

Figure 10 Dissolved [Cl⁻] during the experimental period. Initially [Cl⁻] decreased over time but following week 6 [Cl⁻] increased over time. [Cl⁻] were generally higher in the CR (LG, CRU) than the MR (MRD, MRU).

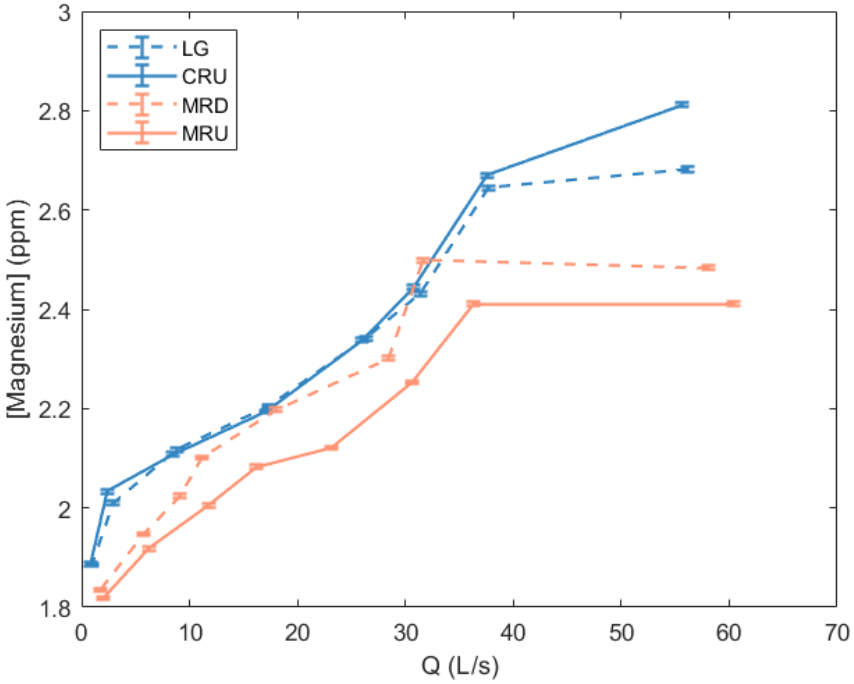

Figure 11 **Mean discharge and dissolved [Mg^{2+}]. Generally [Mg^{2+}] increased monotonically with flow.**

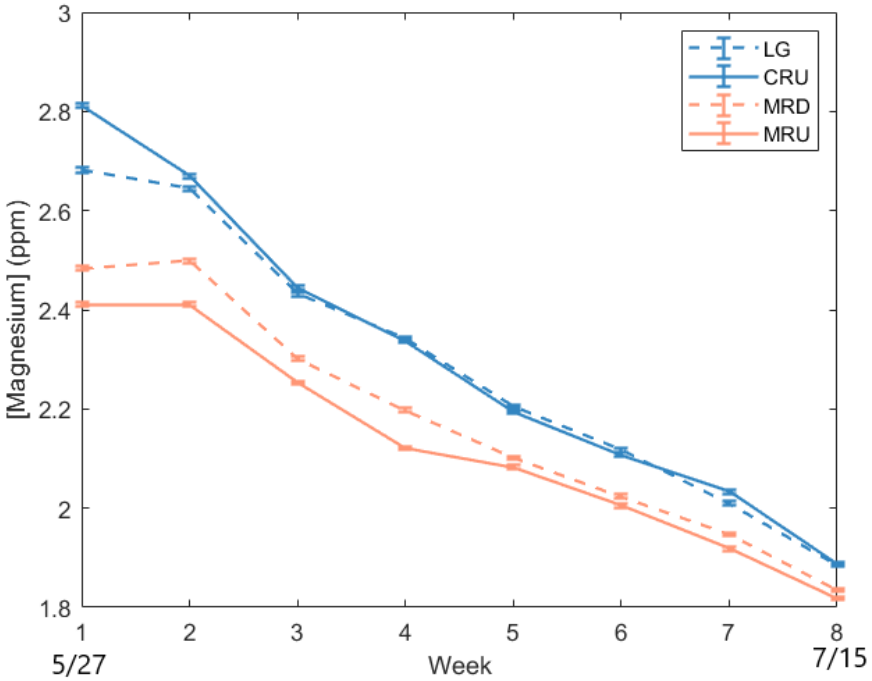

Figure 12 **Dissolved [Mg^{2+}] during the experimental period. [Mg^{2+}] decreased during the experimental period.**

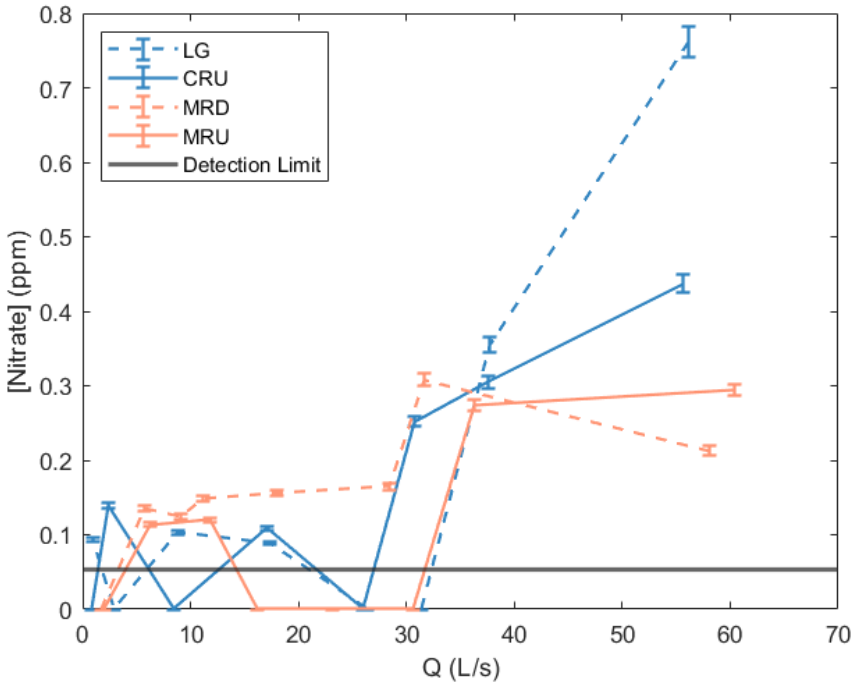

Figure 13 Mean discharge and dissolved [NO_3^-]. Generally [NO_3^-] is higher at MRD than MRU. During high flows [NO_3^-] at LG is higher than MRD, MRU and CRU.

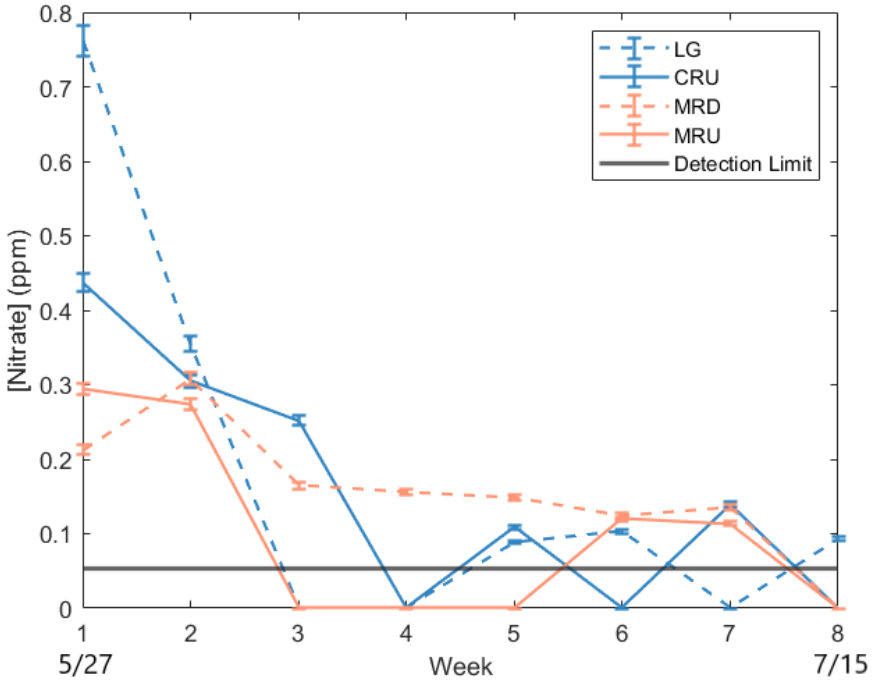

Figure 14 Dissolved [NO_3^-] during the experimental period. Early season [NO_3^-] at LG is higher than MRD, MRU and CRU.

CHAPTER 6: DISCUSSION

6.1 Seasonal Variation in Water Sources to Streamflow are Indicated by the Concentration of Geogenic Solutes

The chemical signature of stream water in the DCEW suggests groundwater and downgradient alluvial flow (DAF) were major sources of water to Dry Creek and that the timing and the relative contribution of groundwater and DAF varies seasonally (Table 8). Groundwater and DAF are transported from subsurface flow paths to Dry Creek by hydraulic gradients. Snowmelt likely promotes infiltration and percolation of water below the vadose zone, which increases the hydraulic gradient between the groundwater table and the stream and enhances groundwater contributions to Dry Creek. As the watershed dries during the summer, infiltration and the hydraulic gradient of the groundwater table is reduced, such that during low summer flows DAF is the primary source of water in Dry Creek.

Table 9 Contextual definitions of groundwater and DAF, their chemical signatures, and derivation of geogenic solutes.

Component	Contextual Definition	Chemical Signature (Solute)	Solute Derivation
Groundwater	Water traveling through deep subsurface flow through unweathered bedrock	Magnesium[1]	Chemical Weathering
Downgradient Alluvial Flow	Water traveling through shallow subsurface flow paths and alluvial fill in the stream	Chloride[2]	Atmospheric Deposition

1. Magnesium is generated in deep subsurface flow paths and the extent of magnesium production and transport to surface water is dependent on vertical hydrologic connectivity and depth to reactive sites (Botter et al., 2020; Xiao et al, 2021).
2. ⅓ of chloride in the DCEW results from wet deposition like precipitation, while the remaining ⅔ results from dry deposition including anthropogenic inputs and eolian transport. Chloride is deposited across the watershed through the year and likely concentrates in the shallow subsurface and alluvial fill (Aishlin & McNamara, 2011).

There was no discernible change between upstream and downstream [Cl^-] in either reach, likely because the reaches were too short to incorporate any local variability in deposition or transport (Hypothesis 1, *p=97.1%*). However, the [Cl^-] trend was nonlinear over time and was consistently higher in the CR than in the MR (Figure 10).

These results suggest that spatiotemporal variability in [Cl^-] is caused by early chloride flushing and late season evapoconcentration in DAF (Raymond et al., 2016). Chloride flushing is the process of dissolving and releasing chloride, that has previously been deposited in the watershed, from the watershed during high spring flows. Chloride is deposited and stored across the watershed throughout the year and likely concentrates in the shallow subsurface and alluvial fill. In Spring, flow through dried areas in the shallow subsurface and alluvial fill is reestablished, and stored chloride is dissolved and transported downgradient. During this time [Cl^-] in the stream are high. As chloride is depleted (e.g., flushed) from the shallow subsurface and alluvial fill, [Cl^-] declines. In Dry Creek the [Cl^-] declined with decreasing flow from May 27th to, approximately, June 17th and July 1st (Hypothesis 2, *p=75.4%*)). From July 1st to July 15th (last 2 weeks of the study period) [Cl^-] began to increase again, likely as a result of rain events or evapoconcentration (Hypothesis 2, *p=65.2%*). Rain events occurred during early June and July and could have caused additional flushing events which may explain increases in [Cl^-] following week 4 and week 7. In this case precipitation would temporally increase downgradient flow picking up and flushing previously deposited Cl from the watershed.

Evapoconcentration occurs when pure water is extracted from the shallow subsurface and alluvial fill by aquatic and riparian vegetation and leaves behind high concentrations of chloride in the stream. During the last two weeks of the study period [Cl^-] was especially susceptible to evapoconcentration, which suggests DAF is the dominant source of water in Dry Creek during low summer flows. Both mechanisms

would also suggest an increase in [Cl^-] downstream because chloride accumulates during flushing and progressively concentrates downgradient from evapoconcentration.

There was a positive relation between flow and [Mg^{2+}] for the entire study period (Figure 11), (Hypothesis 2, *p=99.9%*). This could be the result of temporal changes to the relative contribution of groundwater to streamflow. As discussed above, the relative contribution of groundwater to streamflow is expected to decrease over the course of the study period. This decrease is supported by the monotonic decrease in [Mg^{2+}] and streamflow recorded during the study period.

Future studies should focus on determining the quantity and timing of water release from major water sources (e.g., groundwater and DAF) in lower Dry Creek. I recommend extending the study period to a full year, setting up piezometer nests across and downstream of the MR, and analyzing water samples for natural (e.g., Mg and Cl) and injected tracers (e.g. RWT or KBr). By extending the study period to at least a full year we can track seasonal changes to hydrodynamic conditions and water release from main water sources to streamflow. Piezometer nests can be used, primarily, to collect depth profiles of subsurface water across the MR. By analyzing depth profiles for natural and injected tracers it is possible to determine subsurface flow paths and groundwater contributions to streamflow (Jones et al., 2006). Tracer injections (e.g., RWT or KBr) may also be used to determine hydrologic characteristics like discharge, net storage, and residence time. I also recommend sampling and taking measurements in triplicate to to better quantify sample variability and measurement errors. In combination the proposed methods would quantify seasonal variation in groundwater contribution, flow paths and hydrodynamic conditions.

6.2 Biogeochemical Processing Varies with Seasonal Hydrology

Research suggests beaver meadows can both release and retain NO_3^- depending on the flow condition. Beaver meadows have been shown to retain nutrients at high flows and release nutrients at low flows, but generally beaver meadows are net sinks for NO_3^- (Powers et al., 2012; Wegener et al., 2017). In this study the MR released NO_3^- while flows decreased in the summer (Hypothesis 1, *p=52.2%*) and generally NO_3^- was higher in the beaver meadow than in the control reach (Figure 14).

The reason behind the observed NO_3^- trends in the study are still unclear, but there are a few factors that could influence [NO_3^-] in Dry Creek. NO_3^-could be elevated at MRD because of the immediate upstream environment (Baker et al., 2011; Kamjunke et al., 2020; Stegen et al., 2016). MRD is located just downstream of a beaver dam. Behind the dam is a muddy pond. High levels of organic matter in the pond could yield high organic nitrogen and subsequent production of NO_3^-. If uptake in and around the pond is limited, NO_3^- may be transported downstream to MRD before it is fully assimilated or denitrified. NO_3^- concentrations could also be influenced by cattle, since riparian cattle grazing is known to affect nitrate cycling in montane streams (Hubbard et al., 2004). A dozen or so cattle were known to graze in around Dry Creek especially along the MR during the experimental period. Finally, spatial variation in NO_3^-could result from anthropogenic inputs. The high concentration of NO_3^- at LG in week 1, was likely the result, of a known, septic leak from nearby homes (P. Aishlin, personal communication, March 4th, 2021). NO_3^- may be better transported from the contaminant source during high flows when the hydraulic gradient to the creek is higher and suggests anthropogenic inputs of NO to the DCEW should not be ruled out.

Future studies should focus on relating seasonal hydrodynamic conditions to biogeochemical function in the beaver meadow. I recommend expanding the experimental period to a full year, coninjecting a solute and reactive tracer, setting up piezometer nests around the MR and CR, and analyzing soil and water samples (from stream and piezometer sampling sites) for dissolved oxygen, NO_3^-, ammonium and total nitrogen. A full year incorporates the full cycle of seasonal hydrodynamic and biogeochemical conditions. Solute injections can be used to quantify reach uptake, while reactive tracer injections can be used to quantify reach reactivity (Briggs et al., 2013; Hanrahan et al., 2018; Roche et al., 2019). In combination they may be able separate nutrient uptake (e.g., assimilation) from nutrient removal (e.g., denitrification). Specifically, denitrification rates can be characterized using an injection of 15N labeled NO3 and subsequently measuring dissolved N2 in the stream, and by analyzing streambed sediment samples in the lab for their denitrification potential (Mulholland et al., 2008; Inwood et al., 2007). Conservative tracers could also be used to determine discharge and mean residence time, throughout the year. Piezometer nests can be used to determine vertical advective flux from ground to surface water and collect water profiles (Briggs et al., 2013). By analyzing water profiles and soil samples across the meadow for dissolved oxygen and NO_3^-, we can quantify and map seasonal patterns in oxic conditions and NO_3^- storage and release over longer time periods (e.g., months to years). Again, I would generally recommend sampling and taking measurements in triplicate to improve estimates of sample variability and measurement errors. In combination the proposed methods couple measurement of seasonal hydrodynamic conditions (e.g., flow,

μ, and vertical advective flux) to measurements of spatiotemporal patterns in biogeochemical cycling.

6.3 Evidence of Increased Storage in Reaches with Beaver Activity

The study revealed that net water storage was consistently higher in the beaver meadow than in the control reach. This result corroborates previous research, which has found similar increases in storage, and is evidence that beaver activity increases storage in semi-arid watershed (Puttock et al., 2017). The result also suggests that beaver activity augments water availability during low flows. Net discharge through the beaver meadow was negative, suggesting more water was entering the BM than draining from the MR.

The relationship between seasonal hydrology and variations in water storage in the meadow reach are still, however, unclear and should be explored in future studies. The relationship is important for understanding how susceptible storage in the beaver meadow is to changes in hydrology, and in turn how changes in storage may impact stream flow. I recommend performing tracer injections a few times per week for an entire year. Tracer injections can be used to quantify storage and discharge. Extending the study period to a full year and sampling a few times per week, would incorporate a full spectrum of seasonal changes in storage and streamflow.

CHAPTER 7: CONCLUSION

In this study, I compared the hydrology and water quality of two reaches, one with and one without beaver activity. My original study goals were to expand our understanding of the link between hydrology and biogeochemical function to in turn offer some insight to the historical form and function of Western watersheds and how beaver activity can restore degraded streams.

I hypothesized the beaver meadow would be a nitrate sink and that nitrate retention would decrease monotonically with flow. However, I found the meadow was a net source of NO_3^- during the summer when flows decreased, maybe due to upstream transformation of organic nitrogen deposits within the meadow, or due to livestock grazing. Together with previous research, that shows beaver meadows are a net sink of NO_3^- on annual timescales, my results suggest that nutrient cycling is closely linked to seasonal hydrology and that beaver meadows enhance temporarily dynamic variations in nutrient cycling relative to channels without beaver activity. In this case, beaver activity has implications for the timing and magnitude of nutrient cycling in semi-arid watersheds. Future research is needed to better understand how seasonal hydrology relates to temporal changes in nutrient fluxes within the beaver meadow, as well as the variability in biologically mediated reactions.

I also hypothesized that the concentration of geogenic solutes would decrease monotonically with decreasing flow. The results showed that chloride and magnesium concentrations behaved differently during the experimental period and were therefore

explained by different mechanisms. Both proposed mechanisms relied on the same conceptual model. The conceptual model was based on the assumed chemical signature of groundwater ($[Mg^{2+}]$) and DAF ($[Cl^{-}]$). In the model I propose groundwater and DAF, are major sources of water to Dry Creek and that the relative contribution of each varies temporally. In this case groundwater constitutes a relatively higher proportion of stream water in spring, but low summer flows are predominantly DAF.

$[Cl^{-}]$ started out high and decreased monotonically with flow, but after six weeks $[Cl^{-}]$ began increasing while flows continued to decline. This trend could be a result of chloride flushing in spring and evapoconcentration in summer. $[Mg^{2+}]$ declined throughout the study period and could be a direct consequence of declining groundwater contribution to streamflow.

In the study I also found evidence that beaver activity increased water storage in the meadow reach during low summer flows, when compared to the reach without beaver activity. The result suggests that beaver activity enhances water availability during critical low flow periods in semi-arid watersheds. This has major implications for water supply and drought management in western watersheds. Future research is needed to relate seasonal variation in hydrology and storage in the beaver meadow, which will help determine whether this ecosystem service (i.e., enhanced water storage) is resilient to future changes in the quantity and timing of water release from major water sources (e.g. groundwater and DAF) to semi-arid watersheds in the West.

REFERENCES

Aishlin, P., & McNamara, J. P. (2011). Bedrock infiltration and mountain block recharge accounting using chloride mass balance. *Hydrologic Process.*

Baker, D., Bledsoe, B. P., & Price, J. M. (2011). Stream nitrate uptake and transient storage over a gradient of geomorphic complexity, north-central Colorado, USA. *Hydrological Processes, Vol. 26, Issue 21,* 3241-3252.

Bernhardt, E. S., Hefferman, J. B., Grimm, N. B., Stanley, E. H., Harvey, J. W., Arrolta, M., Appling, A. P., Cohen, M. J., McDowell, W. H., Hall, R. O. Jr., Read, J. S., Roberts, B. J., Stetss, E. G., & Yackulic, C. B. (2017). The metabolic regimes of flowing waters. *Limnology and Oceanography,* 99-118.

Botter, M., Li, L., Hartmann, J., Burlando, P., & Fatichi, S. (2020). Depth of Solute Generation is a Dominant control on Concentration-Discharge Relations. *Water Resource Research, 56.*

Briggs, M. A., Lautz, L. K., Hare, D. K., & González-Pinzón, R. (2013). Relating hyporheic fluxes, residence times, and redox-sensitive biogeochemical processes upstream of beaver dams. *Freshwater Science, Vol. 32, No. 2*, 622-641.

Briggs, M. A., Gooseff, M. N., Arp, C. D., & Baker, M. A. (2009). A method for estimating surface transient storage parameters for streams with concurrent hyporheic storage. *Water Resources Research, 45, W00D27.*

Butler, D. R., & Malanson, G. P. (2005). The geomorphic influences of beaver dams and failures of beaver dams. *Geomorphology, 71(1),* 48-60.

Cardinale B. J., Palmer M., Swan C., Brooks S., & Poff, N. L. (2002). The Influence of Substrate Heterogeneity on Biofilm Metabolism in a Stream Ecosystem. *Ecology, Vol. 83*, 412-422.

Catalan, N., Ortega S. H., Grontoft, H., Hilmarsson, T. G., Bertilsson, S., Wu, P., Levanoni, O., Bishop, K., & Bravo, A. G. (2017). Effects of beaver

impoundments on dissolved organic matter quality and biodegradability in boreal riverine systems. *Hydrobiologia, 793,* 135-148.

Devito, K. J., Dillon, P. J., & Lazerte, B. D. (1989). Phosphorous and nitrogen retention in five Precambrian shield wetlands. *Biogeochemistry, Vol. 8, No. 3,* 185-204.

Ensign, S. H., & Doyle, M. W. (2005). In-channel transient storage and associated nutrient retention: Evidence from experimental manipulations. *Limnology and Oceanography, 50(6),* 1710-1751.

Exner-Kittridge, M., Salinas, J. L., & Zessner, M. (2014). An evaluation of analytical stream to groundwater exchange models: a comparison of gross exchanges based on different spatial flow distribution assumptions. *Hydrology and Earth System Sciences, 18,* 2715-2734.

Fisher, J., & Acreman, M. C. (2004). Wetland nutrient removal: a review of the evidence. *Hydrology and Earth System Sciences, 8(4),* 673-685.

Geisler, E. T. (2015). Riparian Zone Evapotranspitation Using Streamflow Diel Signals. *Boise State University Theses and Dissertations.* 1090.

Godsey, E. S., Hartmann, J., & Kirchner, J. W. (2019). Catchment chemostasis revisted: Water quality responds differently to variation in weather and climate. *Hydrological Processes, Vol. 33, Isue 24,* 3056-3069.

Goldfarb, B. (2018). Eager: The Surprising, Secret Life of Beavers and Why They Matter. *White River Junction, VT: Chelsea Green Publishing.*

Hale, R. B., & Godsey, S. E. (2019). Dynamic stream network intermittence explains emergent dissolved organic carbon chemostasis in headwaters. *Hydrological Processes, 33,* 1926-1936.

Hanrahan, B. R., Tank, J. L., Shogren, A. J., & Rosi, E. J. (2018). Using the raz-rru method to examine linkages between substrate, biofilm colonisation and stream metabolism in open-canopy streams. *Freshwater Biol. 63*, 1610–1624.

Hubbard, R. K., Newton, G. L., & Hill, G. M. (2004). Water Quality and Grazing Animal. *Journal of Animal Science, 2004. 82(13_suppl),* E255-E263.

Inwood, S. E., Tank, J. L., & Bernot, M. J. (2007). Factors Controlling Sediment Denitrification in Midwestern Streams of Varying Land Use. *Microbial Ecology, 53,* 247-258.

Jones, J. P., Sudickey, E. A., Brookfield, A. E., & Park, Y. J. (2006). An assessment of the tracer-based approach to quantifying groundwater contribution to streamflow. *Water Resource Research, Vol. 42, Issue 2.*

Kamjunke, N., Lechtenfeld, O. J., & Herzsprung, P. (2020). Quality of dissolved organic matter driven by autotrophic and heterotrophic microbial processes in a large river. *Water, 12, 1577.*

Karran, J. D., Wesbrook, C. J., & Bedard-Haughn, A. (2018). Beaver-mediated water table dynamics in a Rocky Mountain fen. *Ecohydrology, 2018;11:e1923.*

Kauffman, J. B., & Krueger, W. C. (1984). Livestock impacts on riparian ecosystems and streamside management implications... a review. *Rangeland Ecology & Management/Journal of Range Management Archives, 37(5),* 430-438.

Kilpatrick, F. A., & Wilson, J. F. Jr. (1989). Measurement of time of travel in streams by dye tracing. *US Geological Survey, Book 3, Chapter A9.*

Knapp, J. L. A., Gonzalez-Pinzon, R., Drummond, J. D., Larsen, L. G., Cirpka, O. A., & Harvey, J. W. (2017). Tracer-based characterization of hyporheic exchange and benthic biolayers in streams. *Water Resource Research, 53,* 1575-1594.

Kuypers M. M. M., Marchant, H. K., & Kartal, B. (2018). Thee microbial-cycling network. *Microbial Biogeochemistry, Vol. 18,* 263-276.

Larsen, A., Larsen, J. R., & Lane, S. N. (2021). Dam builders and their works: Beaver influences on the structure and function of river corridor hydrology, geomorphology, biogeochemistry and ecosystems. *Earth-Science Reviews, 218 (2021) 103623.*

Lautz, L., Kelleher, C., Vidon, P., Coffman, J., Riginos, C., & Copeland, H. (2019). Restoring stream ecosystem function with beaver dam analogues: Let's not make the same mistake twice. *Hydrologic Processes,* 33, 174-177.

Lewandowski, K., Arnon, S., Banks, E., Baelaan, O., Betterle, A., Broecker, T., Coll, C., Drummond, J. D., Garcia, J. G., Galloway, J., Gomez-Velez, J., Grabowski, R. C., Herzog, S. P., Hinkelmann, R., Höhne, A., Hollender, J., Horn, M. A., Jaeger, A., Krause, S.,…Wu, L. (2019). Is the hyporheic zone relevant beyond the Scientific Community. *Water, 11, 2230.*

Lurry, D., & Kolbe, C. (2000). Interagency Field Manual for the Collection of Water-Quality Data. *US Geological Survey, 00-213.*

Lynch, L., Sutfin, N., Fegel, T., Boot, C., Covino, T., & Wallenstein, M. (2019). River channel connectivity shifts metabolite composition and dissolved organic matter chemistry. *Nature Communications.*

Majerova, M., Beilson, B. T., Schmadel, N. M., Wheaton, J. M., & Snow, C. J. (2015). Impacts of beaver dams on hydrologic and temperature regimes in a mountain stream. *Hydrology and Earth System Sciences, 19,* 3541-3556.

Malakoff, D. (2004). The River Doctor. *Science, Vol. 305, No. 5686,* 937-939.

McNamara, J., & Aishlin, P. (2017). *Lower Gauge: Stream Data from Dry Creek Experimental Watershed.* Department of Geosciences, Boise State University. Watershed Process Research Group. Web. 14 August 2021.

McNamara, J., & Aishlin, P. (2018). *Lower Gauge: Stream Data from Dry Creek Experimental Watershed.* Department of Geosciences, Boise State University. Watershed Process Research Group. Web. 14 August 2021.

McNamara, J., & Aishlin, P. (2019). *Lower Gauge: Stream Data from Dry Creek Experimental Watershed.* Department of Geosciences, Boise State University. Watershed Process Research Group. Web. 14 August 2021.

McNamara, J., & Aishlin, P. (2020). *Lower Gauge: Stream Data from Dry Creek Experimental Watershed.* Department of Geosciences, Boise State University. Watershed Process Research Group. Web. 13 August 2021.

McIntosh, J. C., Scaumberg, C., Perdrial, J., Harpold, A., Vazques-Ortega, A., Rasmussen, C., Vinson, D., Zapata-Rios, X., Brooks, P. D., Meixner, T., Pelletier, J., Derry, L., & Chorover, J. (2017) Geochemical evolution of the Critical Zone across variable time scales informs concentration-discharge relationships: Jemez River Basin Critical Zone Observatory. *Water Resource Research, Vol. 53, Issue 5,* 4169-4196.

Mulholland, P. J., Helton, A. M., Poole, G. C., Hall, R. O., Hamilton, S. K., Peterson, B. J., Tank, J. L., Ashkenas, L. R., Cooper, L. W., Dahm, C. N., Dodds, W. K., Findlay, S. E. G., Gregory, S. V., Grimm, N. B., Johnson, S. L., McDowell, W. H., Meyer, J. L., Valett, H. M., Webster, J. R…Thomas, S. M. (2008). Stream

denitrification across biomes and its response to anthropogenic nitrate loading. *Nature, 452,* 202-205.

Naiman, R. J., Johnston, C. A., & Kelley, J. C. (1988). Alterations of North American Streams by Beaver. *BioScience, Vol. 38, No. 11,* 753-762.

Nogaro, G., Datry, T., Memillod-Blondin, F., Fouldquier, A., & Montuelle, B. (2013). Influence of hyporheic zone characteristics on the structure and activity of microbial assemblages. *Freshwater Biology, 58,* 2567-2583.

Nyssen, J., Pontzeele J., & Billi, P. (2011). Effect of beaver dams on the hydrology of small mountain streams: Example from the Chevral in the Ourthe Orientale basin, Ardennes, Belgium. *Journal of Hydrology, 402,* 92-102.

Palmer, M., & Ruhl, A. (2019) Linkages between flow regime, biota, and ecosystem processes: Implications for river restoration. *Science,* 365 (6459).

Payn, R. A., Gooseff, M. N., McGlynn, B. L., Bencala, K. E., & Wondzell, S. M. (2009). Channel water balance and exchange with subsurface flow along a mountain headwater stream in Montana, United States. *Water Resources Research, Vol. 45, W11427.*

Pollock, M. M., Beechie, T. J., Wheaton, J. M., Jordan, C. E., Bouwes, N., Weber N., & Volk, C. (2014). Using Beaver Dams to Restore Incised Stream Ecosystems. *BioScience, Vol. 64, No. 4,* 279-290.

Powers, S. M., Johnson, R. A., & Stanley, E. H. (2012). Nutrient Retention and the Problem of Hydrologic Disconnection in Streams and Wetlands. *Ecosystems (2012) 15,* 435-449.

Puttock, A., Graham, H. A., Cunliffe, A. M., Elliot, M., & Brazier, R. E. (2017). Eurasian beaver activity increases water storage, attenuates flow and mitigates diffuse pollution from intensively-managed grasslands. *Science of Total Environment, 576 (2017),* 430-443.

Raymond, P. A., Saiers, J. E., & Sobczak, W. V. (2016). Hydrological and biogeochemical controls on watershed dissolved organic matter transport: pulse-shunt concept. *Ecology, Vol. 97, No. 1.* 5-16.

Roche, K. R., Shogren, A. J., Aubeneau, A., Tank, J. L., & Bolster, D. (2019). Modeling benthic versus hyporheic nutrient uptake in unshaded streams with varying substrates. *Journal of Geophysical Research: Biogeosciences, 124.*

Rosgen, D. L. (1994). A classification of natural rivers. *Catena, 22,* 169-199.

Stegen, J. C., Frederickson, J. K., Wilkins, M. J., Konopka, A. E., Nelson, W. C., Arntzen, E. V., Chrisler, W. B., Chu, R. K., Danczak, R. E., Fransler, S. J., Kennedy, D. W., Resch, C. T., & Tfaily, M. (2016). Groundwater-surface water mixing shifts ecological assembly processes and stimulates organic carbon turnover. *Nature Communications, 7:11237.*

Tonina, D., & Buffington, J. M. (2009). Hyporheic Exchange in Mountain Rivers|: Mechanics and Environmental Effects. *Geography Compass 3/3 (2009),* 1063-1086.

Turnipseed, D. P., & Sauer, V. B. (2010). Discharge measurements at gaging stations. *US Geological Survey. No. 3-A8.*

Vitousek, P. M., Aber, J. D., Howarth, R. W., Likens, G. E., Matson, P. A., Schindler, D. W., Schleisinger, W. H., & Tilman, D. G. (1997). Human Alteration of the Global Nitrogen Cycle: Sources and Consequences. *Ecological Applications 7(3), 1997,* 737-750,

Wade, J., Lautz, L., Kelleher, C., Vidon, P., Davis, J., Beltran, J., & Pearce, C. (2020). Beaver dam analogues drive heterogeneous groundwater-surface water interactions. *Hydrological Processes,* 1-14.

Wegener, P., T. Covino, & E. Wohl (2017), Beaver-mediated lateral hydrologic connectivity, fluvial carbon and nutrient flux, and aquatic ecosystem metabolism, *Water Resources Research, 53,* 4606–4623.

Westbrook, C. J., Cooper, D. J., & Baker, B. W. (2005). Beaver dams and overbank floods influence groundwater-surface water interactions of a Rocky Mountain riparian area. *Water Resources Research, Vol. 42, W06404.*

Wohl, E. (2005). Compromised Rivers: Understanding Historical Human Impacts of Rivers in the Context of Restoration. *Ecology and Society, Vol. 10, No. 2.*

Wohl, E., & Beckman, N. D. (2014). Leaky rivers: Implications of the loss of longitudinal fluvial disonnectivity headwater streams. *Geomorphology, 205,* 27-35.

Worrall, F., Howden, N. J. K., & Burt, T. P. (2014). A method of estimating in-stream residence time of water in rivers. *Journal of Hydrology, 512,* 274-284.

Xiao, D., Brantley, S. L., & Li, L. (2021). Vertical Connectivity Regulates Water Transit Time and Chemical Weathering at Hillslope Scale. *Water Resources Research, Vol. 57, Issue 8.*

Yu-Chen Lin, A., Debroux, J. F., Cunningham, J. A., & Reinhard, M. (2003). Comparison of rhodamine WT and bromide determination of hydraulic characteristics of constructed wetlands. *Ecological Engineering, 20.1,* 75-88.

APPENDIX A

Calculations

IC Detection Limits

Detection limits (DL) were applied to the IC results for magnesium, chloride, and nitrate. They were determined using the area of the IC curves for each ion established by the Metrohm MagICNet Software. Calibration curves and related data were established using a set of standards. Calculation of the DL for each ion is shown herein. The follow equations were used to calculate the detection limits.

$$DL = \frac{3.3 * \sigma}{s}$$

Where σ is the standard deviation of the response and s is the slope of the calibration curve.

$$s = \frac{\sum(Response)^2}{n - 2}$$

Where the Response is the difference between the calibration standard concentration and the measured concentrations and n is the number of standards.

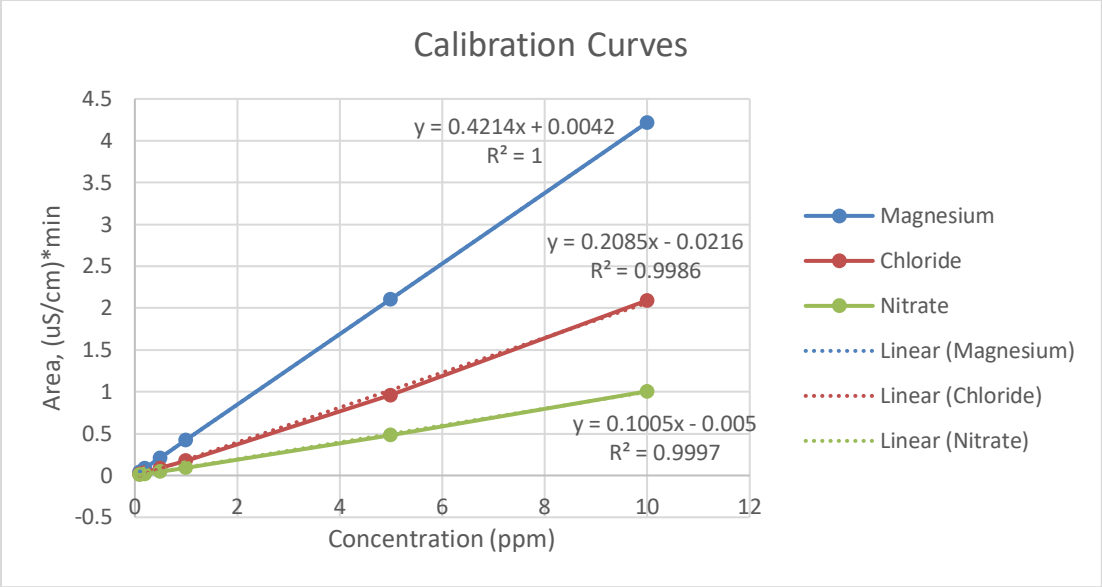

Figure A1 Plot of the IC calibration curves for magnesium, chloride, and nitrate.

Table A1 Calculation of the ion chromatograph's detection limit.

Magnesium				
Standard	[Standard]	Measured Area	[Measure]	([Standard]-[Measured])^2
	ppm	(uS/cm)*min	ppm	
1	0.1	0.045	0.097	0.000
2	0.2	0.091	0.206	0.000
3	0.5	0.213	0.495	0.000
4	1	0.427	1.003	0.000
5	5	2.11	4.997	0.000
6	10	4.219	10.002	0.000
Sum				0.000
Detection Limit	**0.003357189**			
Chloride				
Standard	[Standard]	Measured Area	[Measured]	([Standard]-[Measured])^2
	ppm	(uS/cm)*min	ppm	
1	0.1	0.017	0.185	0.007
2	0.2	0.035	0.271	0.005
3	0.5	0.088	0.526	0.001
4	1	0.178	0.957	0.002
5	5	0.963	4.722	0.077
6	10	2.093	10.14	0.020
Sum				0.112
Detection Limit	**0.119181827**			
Nitrate				
Standard	[Standard]	Measured Area	[Measured]	([Standard]-[Measured])^2
	ppm	(uS/cm)*min	ppm	
1	0.1	0.009	0.139	0.002
2	0.2	0.018	0.229	0.001
3	0.5	0.047	0.517	0.000
4	1	0.093	0.975	0.001
5	5	0.485	4.876	0.015
6	10	1.006	10.06	0.004
Sum				0.022
Detection Limit	**0.053195654**			

Mean Residence Time in CR (Week 8)

Mean residence time within the CR on week 8 was estimated using Manning's equation (Worrall et al., 2014). The following equations were used to calculate μ at CRU on week 8:

$$V = \left(\frac{1}{n}\right)\left(\frac{D * W}{2(D + w)}\right)^{\frac{2}{3}}(s)^{\frac{1}{2}}$$

$$\mu = V/L$$

Where V is the main channel discharge velocity, n is Manning's roughness coefficient, D is the depth of water, W is the average reach width, S is the reach bedslope based on length of reach and upstream and downstream elevations*, and L is the reach length.

The depth of water was calculated using the established rating curve for LG provided by the Boise State University Department of Geosciences. The rating curve equation was:

$$0.282Q^{0.304}$$

In this case I used the average flow through CR on weeks 2, 5 and 8 for Q.

Given:

1. Bedslope (S) = 0.038759 m/m
2. Length of Reach (L)* = 232.33 m
3. Average Reach Width = 1 m
4. n = Adjusted to match values for recorded μ. Used linear interpolation of depth and n for week 8.

Table A2 Calculation of the mean residence time in CR.

Width	1	m					
Week	LG Q	CRU Q	Avg Q	Depth	Roughness (n)	V	μ
	(L/s)	(L/s)	(L/s)	(m)		(m/s)	(min)
2	37.67	37.64	37.65	0.09	0.32	0.11	34.31
5	17.31	17.02	17.17	0.07	0.45	0.07	55.04
8	0.90	0.84	0.87	0.03	0.73	0.02	155.76
Width	1.5	m					
Week	LG Q	CRU Q	Avg Q	Depth	Roughness (n)	V	μ
	(L/s)	(L/s)	(L/s)	(m)		(m/s)	(min)
2	37.67	37.64	37.65	0.09	0.33	0.11	34.31
5	17.31	17.02	17.17	0.07	0.46	0.07	55.04
8	0.90	0.84	0.87	0.03	0.72	0.03	151.64
Width	0.5	m					
Week	LG Q	CRU Q	Avg Q	Depth	Roughness (n)	V	μ
	(L/s)	(L/s)	(L/s)	(m)		(m/s)	(min)
2	37.67	37.64	37.65	0.09	0.29	0.11	34.31
5	17.31	17.02	17.17	0.07	0.41	0.07	55.04
8	0.90	0.84	0.87	0.03	0.66	0.03	145.80

*Obtained from Google Earth Pro, 2019.

Gross Gains and Losses

The calculated GG for the MR in weeks 2 and 5 was negative indicating a data collection error. The error is likely the result of incomplete mixing, especially at MRD. Incomplete mixing of KBr is assumed to yield an under-estimation of Q in the channel. To determine the effect of incomplete mixing on GG, I calculated the GG given three scenarios. I assumed incomplete mixing would result in a higher concentration of mass passing the Sonde, to mimic this effect I adjusted the KBr values by 10 grams in each scenario. In the first scenario, I assumed incomplete mixing at MRD and increased KBr mass at MRD, in the second scenario I assumed incomplete mixing at MRU and increased KBr at MRU, and in the third scenario I assumed incomplete mixing at both MRU and MRD and increased KBr masses at both sites. I then calculated discharge (Q) and *f* using the sonde data and the adjusted KBr values. Q and *f* were then used to calculate GG for each scenario.

The following equations were used to calculate gross gains and losses:

$$Gross\ Gain = Q_{down} - Q_{up} + Q_{avg}(1 - f)$$

$$Gross\ Loss = Q_{avg}(1 - f)$$

where Q_{down} is the downstream reach discharge, Q_{up} is the upstream reach discharge, Q_{avg} is the average of Q_{down} and Q_{up} and f is the fraction of RWT mass recovered. The fraction of RWT mass recovered (f) was calculated using:

$$f = \frac{Q_{avg} \int RWT}{(\frac{Mass}{5})}$$

where $\int$ RWT is the integral of the RWT breakthrough curve and $\frac{\text{Mass}}{5}$ is the mass of 20% (wt/wt) Rhodamine solution used for the RWT injection.

Table A3 Calculation of the gross gains and losses to search for sources of error.

	Measured	MRD Adjusted	MRU Adjusted	Both Adjusted
KBr Mass at MRD (g)	100.6	110.6	100.6	110.6
KBr Mass at MRU (g)	99.8	99.8	109.8	109.8
MRD Q (L/s)	31.7	34.9	31.7	34.9
MRU Q (L/s)	36.3	36.3	40.0	40.0
Average Q (L/s)	34.0	35.6	35.8	37.4
f	0.9	0.9	1.0	1.0
Gross Loss (L/s)	3.3	1.9	1.7	0.2
Gross Gain (L/s)	-1.3	0.5	-6.6	-4.9

Table 11 shows that only when KBr was adjusted at MRD did I end up with a positive GG value. This suggests that incomplete mixing at MRD was the most likely source of error.

KBr Conductivity Scaling Factor

A scaling factor is necessary to convert conductivity to concentration. This was done by first adding a known mass of KBr to a known volume of stream water. The concentration of the solution was calculated, and the conductivity was then measured using the EXO 3 Sonde. The slope of the concentration-conductivity line is the scaling factor.

Table A4 Calculation of the KBr scaling factor.

Volume H2O (mL)	Mass KBr (g)	Sonde (uS/cm)	Theoretical (uS/cm)	Concentration (mg/L = ppm)
500	0	150.9	150.0	0
500	0.047	280.0	244.0	94
500	0.0835	387.9	317.0	167

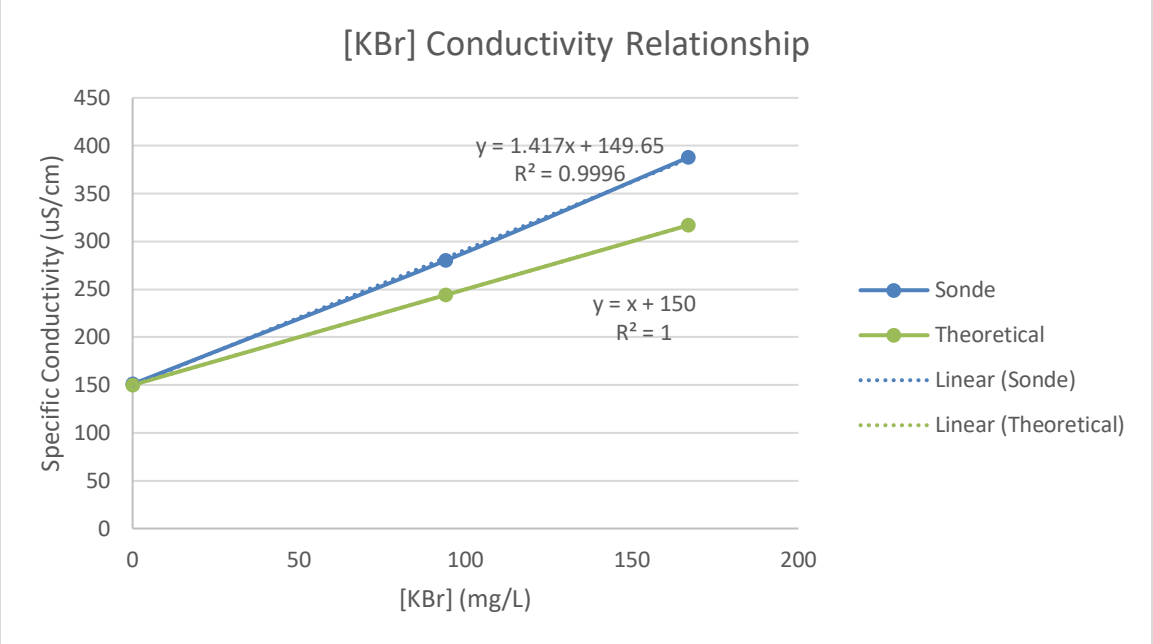

Figure A2 Plot of the theoretical and measured KBr concentration and conductivity with associated linear trend lines.

APPENDIX B

Statistical Analysis

Table B1 Hypothesis 1 Chloride Testing

Hypothesis 1: Chloride Statistics		
There is no change in chloride concentrations between the upstream and downstream sampling sites within each reach.		
Null Hypothesis	x=0	
Test Hypothesis	x>0; x<0	
[Cl] in Meadow Reach (ppm)		
MRU	MRD	MRD-MRU
1.687	1.388	-0.299
1.216	1.236	0.02
1.227	1.231	0.004
1.139	1.155	0.016
1.222	1.238	0.016
1.193	1.199	0.006
1.317	1.32	0.003
1.456	1.707	0.251

Statistics		
X	0.002125	*Mean of (MRD-MRU)*
S	0.14800525	*Standard deviation of the sample*
T.Stat	0.03798664	*T statistic where $\mu=0$*
P Value	0.97076	*Two tailed t statistic*
t	2.365	*t for 95% two-sided CI*
CI UB	0.35215741	*Upper bound of confidence interval*
CI LB	-0.3479074	*Lower bound of confidence interval*

97.1 % chance there is no difference between upstream and downstream [Cl] in MR.

[-0.35, 0.35] 95% confidence interval of difference between LG and CRU.

Instrument error from IC suggests there is no difference between upstream and downstream [Cl]

[Cl] in Control Reach (ppm)		
CRU	LG	LG-CRU
1.912	1.87	-0.042
1.699	1.668	-0.031
1.535	1.544	0.009
1.375	1.39	0.015
1.386	1.393	0.007

1.349	1.347	-0.002
1.427	1.421	-0.006
1.556	1.552	-0.004

Statistics		
X	0.00675	*Mean of (MRD-MRU)*
S	0.01989795	*Standard deviation of the sample*
T.Stat	0.89752049	*T statistic where $\mu=0$*
P Value	0.399257	*Two tailed t statistic*
t	2.365	*t for 95% two-sided CI*
CI UB	0.05380866	*Upper bound of confidence interval*
CI LB	-0.0403087	*Lower bound of confidence interval*

39.9% chance there is no difference between upstream and downstream [Cl] in CR.

[0.040, 0.054] 95% confidence interval of difference between LG and CRU [Cl].

Instrument error from IC suggests there is no difference between upstream and downstream [Cl]

Table B2 Hypothesis 1 Magnesium Testing

Hypothesis 1: Magnesium Statistics		
There is no change in Mg concentrations between the upstream and downstream sampling sites within each reach.		
Null Hypothesis	x=0	
Test Hypothesis	x>0; x<0	
[Mg] in Meadow Reach (ppm)		
MRU	MRD	MRD-MRU
2.41	2.484	0.074
2.41	2.499	0.089
2.253	2.301	0.048
2.121	2.198	0.077
2.083	2.101	0.018
2.005	2.024	0.019
1.918	1.948	0.03
1.818	1.834	0.016
Statistics		
X	0.046375	*Mean of (MRD-MRU)*
S	0.02991864	*Standard deviation of the sample*
T.Stat	4.101012559	*T statistic where μ=0*
P Value	0.00456722	*Two tailed t statistic*
t	2.365	*t for 95% two sided CI*
CI UB	0.117132583	*Upper bound of confidence interval*
CI LB	-0.02438258	*Lower bound of confidence interval*
0.46 % chance there is no difference between upstream and downstream [Mg] in MR. [-0.024, 0.12] 95% confidence interval of difference between LG and CRU.		
[Mg] in Control Reach (ppm)		
CRU	LG	LG-CRU
2.812	2.682	-0.13
2.67	2.645	-0.025
2.444	2.432	-0.012
2.338	2.342	0.004
2.194	2.205	0.011
2.108	2.117	0.009
2.033	2.01	-0.023
1.887	1.885	-0.002
Statistics		
X	-0.021	*Mean of (MRD-MRU)*
S	0.046124056	*Standard deviation of the sample*

T.Stat	-1.20459435	*T statistic where μ=0*
P Value	0.267502415	*Two tailed t statistic*
t	2.365	*t for 95% two-sided CI*
CI UB	0.088083393	*Upper bound of confidence interval*
CI LB	-0.13008339	*Lower bound of confidence interval*

26.7% chance there is no difference between upstream and downstream [Mg] in CR. [-0.13, .088] 95% confidence interval of difference between LG and CRU [Mg].

Table B3 Hypothesis 1 Nitrate Testing

Hypothesis 1: Nitrate Statistics

*First test whether downstream NO3 concentrations are less than upstream NO3 concentrations

Null Hypothesis	x=>0
Test Hypothesis	x<0

[NO3] in Meadow Reach (ppm)

MRU	MRD	MRU-MRD
0.294	0.213	0.081
0.274	0.308	-0.034
0	0.165	-0.165
0	0.156	-0.156
0	0.149	-0.149
0.12	0.124	-0.004
0.114	0.136	-0.022
0	0	0

Statistics		
X	-0.056125	*Mean of (MRU-MRD)*
S	0.0900626	*Standard deviation of the sample*
T.Stat	-1.648774	*T statistic where μ=0*
P Value	0.14318	*Two tailed t statistic*
P Value	0.4784053	*Left tailed t statistic*
P Value	0.52159	*Right tailed t statistic*
t	2.365	*t for 95% two sided CI*
CI UB	0.156873	*Upper bound of confidence interval*
CI LB	-0.269123	*Lower bound of confidence interval*

47.8% chance MRU [NO3] is higher than MRD [NO3].
52.2% chance MRD [NO3] is higher than MRU [NO3].
Instrument error from IC suggests there is no difference between upstream and downstream [Cl]

[NO3] in Control Reach (ppm)

CRU	LG	CRU-LG
0.437	0.762	-0.325
0.305	0.355	-0.05
0.252	0	0.252
0	0	0
0.109	0.089	0.02
0	0.103	-0.103
0.14	0	0.14

	0	0.093	-0.093
Statistics			
X		0.019875	*Mean of (CRU-LG)*
S		0.1722651	*Standard deviation of the sample*
T.Stat		0.3052522	*T statistic where μ=0*
P Value		0.7690508	*Two tailed t statistic*
P Value		0.5076511	*Left tailed t statistic*
P Value		0.49235	*Right tailed t statistic*
t		2.365	*t for 95% two sided CI*
CI UB		0.427282	*Upper bound of confidence interval*
CI LB		-0.387532	*Lower bound of confidence interval*

49.2% chance CRU [NO3] is higher than LG [NO3].
50.8% chance LG [NO3] is higher than MRU [NO3].
Instrument error from IC suggests there is no difference between upstream and downstream [Cl]
There is a larger decrease in [NO3] from upstream to downstream sites in the MR than the CR.

Null Hypothesis	x=<CR	x = change in meadow reach
Test Hypothesis	x>CR	

[NO3] (ppm)		
	MRD-MRU	LG-CRU
	0.081	0.325
	0.034	0.05
	0.165	-0.252
	0.156	0
	0.149	-0.02
	0.004	0.103
	0.022	-0.14
	0	0.093
X	0.076375	0.01988
S	0.071027	0.17227
Statistics		
T.Stat	0.8022449	*Two sample T statistic*
P Value	0.22439	*Right tail t statistic*
P Value	0.7756071	*Left tail t statistic*
P Value	0.4487857	*Two tail t statistic*

44.9% chance there is no difference in nitrate reduction between MR and CR.
22.4% chance there is a greater reduction in [NO3] in MR than CR
77.56% chance there is a greater reduction in [NO3] in CR than MR

Table B4 Hypothesis 2 Discharge Testing

Hypothesis 2: Discharge Statistics			
Q decreases over time.			
Null Hypothesis	x=>0		
Test Hypothesis	x<0		
Q in Meadow Reach (L/s)			
Q CR	Q MR	Average Q	dt
55.84	59.22	57.53	
37.65	34	35.825	21.705
31.07	29.53	30.3	5.525
26.14	20.56	23.35	6.95
17.17	12.65	14.91	8.44
8.6	10.38	9.49	5.42
2.62	5.99	4.305	5.185
0.87	1.85	1.36	2.945
Statistics			
X	8.024286	*Mean of (MRD-MRU)*	
S	6.263363	*Standard dev. of the sample*	
T.Stat	3.138155	*T statistic where μ=0*	
P Value	0.01006	*Right tail t statistic*	
P Value	0.989943	*Left tail t statistic*	
P Value	0.020115	*Two tail t statistic*	
t	2.447	*t for 95% two-sided CI*	
CI UB	23.35073	*Upper bound of confidence interval*	
CI LB	-7.30216	*Lower bound of confidence interval*	

If positive then decreasing over time
x = Week 1 - Week 2 [Mg]
x = Week 1 - Week 2 [Mg]

2.01% chance that Q does not changes over time
99% chance that Q decreases over time

Table B5 Hypothesis 2 Chloride and Magnesium Testing

Hypothesis 2: Magnesium and Chloride Statistics

[Mg] increases over time in the MR. [Cl] increases over time in the MR.

Null Hypothesis x=<0

Test Hypothesis x>0

[Mg] in Meadow Reach (ppm)

MRU	MRD	Average	dQ
2.41	2.484	2.447	
2.41	2.499	2.4545	-0.015
2.253	2.301	2.277	0.355
2.121	2.198	2.1595	0.235
2.083	2.101	2.092	0.135
2.005	2.024	2.0145	0.155
1.918	1.948	1.933	0.163
1.818	1.834	1.826	0.214
			If positive then decreasing over time
			x = Week 1 - Week 2 [Mg]

Statistics

X	0.177429	*Mean of dQ*
S	0.112342	*Standard dev. of the sample*
T.Stat	3.868645	*T statistic where μ=0*
P Value	0.00414	*Right tail t statistic*
P Value	0.995861	*Left tail t statistic*
P Value	0.008279	*Two tail t statistic*
t	2.447	*t for 95% two sided CI*
CI UB	0.452328	*Upper bound of confidence interval*
CI LB	-0.09747	*Lower bound of confidence interval*

0.83% chance that [Mg] does not change over time

99.6% chance that [Mg] decreases over time

[-0.097, 0.45] Confidence interval of difference between LG and CRU.

[Mg] in Control Reach (ppm)

CRU	LG	Average	dQ
2.812	2.682	2.747	
2.67	2.645	2.6575	0.179
2.444	2.432	2.438	0.439
2.338	2.342	2.34	0.196
2.194	2.205	2.1995	0.281

2.108	2.117	2.1125	0.174
2.033	2.01	2.0215	0.182
1.887	1.885	1.886	0.271

If positive then decreasing over time
x = Week 1 - Week 2 [Mg]

Statistics		
X	0.246	*Mean of dQ*
S	0.096062	*Standard dev. of the sample*
T.Stat	6.272735	*T statistic where μ=0*
P Value	0.00038	*Right tail t statistic*
P Value	0.999619	*Left tail t statistic*
P Value	0.000763	*Two tail t statistic*
t	2.447	*t for 95% two sided CI*
CI UB	0.481065	*Upper bound of confidence interval*
CI LB	0.010935	*Lower bound of confidence interval*

0.076% chance that [Mg] does not change over time
99.9% chance that [Mg] decreases over time
[0.011, 0.48] Confidence interval of difference between LG and CRU.

[Cl] increases over time in the MR. Q decreases over time in the MR.

Cl		Q	
Null Hypothesis	x=<0	Null Hypothesis	x=>0
Test Hypothesis	x>0	Test Hypothesis	x<0

[Cl] in Meadow Reach (ppm)
Initial Descrease over time = Week 1 to Week 5

MRU	MRD	Average	dQ
1.687	1.388	1.5375	
1.216	1.236	1.226	0.623
1.227	1.231	1.229	-0.006
1.139	1.155	1.147	0.164
1.222	1.238	1.23	-0.166

Statistics		
X	0.15375	*Mean of dQ*
S	0.340617	*Standard dev. of the sample*
T.Stat	0.781824	*T statistic where μ=0*
P Value	0.24567	*Right tail t statistic*
P Value	0.75433	*Left tail t statistic*
P Value	0.491347	*Two tail t statistic*

t	3.182	*t for 95% two sided CI*
CI UB	0.511221	*Upper bound of confidence interval*
CI LB	-0.20372	*Lower bound of confidence interval*

[Cl] in Meadow Reach (ppm)
Late season increase over time = Week 5 to Week 8

MRU	MRD	Average	dt
1.193	1.199	1.196	0.068
1.317	1.32	1.3185	-0.245
1.456	1.707	1.5815	-0.526

Statistics

X	-0.23433	*Mean of (MRD-MRU)*
S	0.297144	*Standard dev. of the sample*
T.Stat	-1.11528	*T statistic where μ=0*
P Value	0.80962	*Right tail t statistic*
P Value	0.190384	*Left tail t statistic*
P Value	0.380769	*Two tail t statistic*
t	4.303	*t for 95% two sided CI*
CI UB	1.044276	*Upper bound of confidence interval*
CI LB	-1.51294	*Lower bound of confidence interval*

[Cl] in Meadow Reach (ppm)
Entire Study Period

MRU	MRD	Average	dt
1.687	1.388	1.5375	
1.216	1.236	1.226	0.623
1.227	1.231	1.229	-0.006
1.139	1.155	1.147	0.164
1.222	1.238	1.23	-0.166
1.193	1.199	1.196	0.683
1.317	1.32	1.3185	-0.245
1.456	1.707	1.5815	-0.526

Statistics

X	0.075286	*Mean of (MRD-MRU)*
S	0.448355	*Standard dev. of the sample*
T.Stat	0.411307	*T statistic where μ=0*
P Value	0.34757	*Right tail t statistic*
P Value	0.652433	*Left tail t statistic*
P Value	0.695135	*Two tail t statistic*
t	2.447	*t for 95% two sided CI*
CI UB	1.17241	*Upper bound of confidence interval*

CI LB	-1.02184	*Lower bound of confidence interval*

69.5% chance that [Cl] does not changes over time
75.4% chance there was an initial decrease in [Cl] in the MR from Week 1 to week 5
65.2% chance that there was a late season increase in [Cl] in the MR from week 5 to week 8.

[Cl] in Control Reach (ppm)

CRU	LG	Average	dQ
1.687	1.388	1.5375	
1.216	1.236	1.226	0.623
1.227	1.231	1.229	-0.006
1.139	1.155	1.147	0.164
1.222	1.238	1.23	-0.166
1.193	1.199	1.196	0.068
1.317	1.32	1.3185	-0.245
1.456	1.707	1.5815	-0.526
			If positive then decreasing over time
			x = Week 1 - Week 2 [Mg]

Statistics

X	-0.01257	*Mean of dQ*
S	0.36121	*Standard dev. of the sample*
T.Stat	-0.08525	*T statistic where $\mu=0$*
P Value	0.53258	*Right tail t statistic*
P Value	0.467418	*Left tail t statistic*
P Value	0.934835	*Two tail t statistic*
t	2.447	*t for 95% two sided CI*
CI UB	0.871309	*Upper bound of confidence interval*
CI LB	-0.89645	*Lower bound of confidence interval*

93.5% chance that [Cl] does not change over time
46.7% chance that [Cl] decreases over time
[-0.90, 0.87] Confidence interval of difference between LG and CRU.